VARIATIONS IN NEARSHORE BAR MORPHOLOGY: IMPLICATIONS FOR RIP CURRENT DEVELOPMENT AT PENSACOLA BEACH, FLORIDA FROM 1951 TO 2004

A Thesis

by

GEMMA ELIZABETH BARRETT

Submitted to the Office of Graduate Studies of
Texas A&M University
in partial fulfillment of the requirements for the degree of

MASTER OF SCIENCE

August 2011

Major Subject: Geography

Variations in Nearshore Bar Morphology: Implications for Rip Current Development at Pensacola Beach, Florida from 1951 to 2004

VARIATIONS IN NEARSHORE BAR MORPHOLOGY: IMPLICATIONS FOR RIP CURRENT DEVELOPMENT AT PENSACOLA BEACH, FLORIDA FROM 1951 TO 2004

A Thesis

by

GEMMA ELIZABETH BARRETT

Submitted to the Office of Graduate Studies of
Texas A&M University
in partial fulfillment of the requirements for the degree of

MASTER OF SCIENCE

Approved by:

Chair of Committee,	Christopher Houser
Committee Members,	Steven Quiring
	John R. Giardino
	Douglas Sherman
Head of Department,	Vatche Tchakerian

August 2011

Major Subject: Geography

ABSTRACT

Variations in Nearshore Bar Morphology: Implications for Rip Current Development at Pensacola Beach, Florida from 1951 to 2004. (August 2011)

Gemma Elizabeth Barrett, B.S., Texas A&M University

Chair of Advisory Committee: Dr. Christopher Houser

In 2002, Pensacola Beach was identified by the United States Lifesaving Association as being the most hazardous beach in the continental United States for beach drowning by rip currents. Recent studies suggest that the rip currents at Pensacola Beach are associated with a transverse bar and rip morphology that develops with the migration of the bars and recovery of the beachface following an extreme storm. Combined with an alongshore variation in wave forcing by transverse ridges on the inner-shelf, the bar cycle (of bar response and recovery to extreme storms) is hypothesized to create both rip current hotspots and periods of rip activity. However, it is unknown at what stage, or stages, the bar cycle is associated with the formation of these hotspots and the greatest number of rips. To determine how the accretional rip hazard varies in response to the nearshore bar cycle, this thesis will quantify the alongshore variation in the nearshore bar morphology on Santa Rosa Island from 1951 to 2004. Aerial photographs and satellite images are collected for the study area and nearshore features are digitized in ArcGIS and evaluated using wavelet analysis. Specifically, a continuous wavelet transform is used to the identify times and locations when a transverse bar and rip

morphology is present or is in the process of developing. The findings suggest that the rip-scale variation in bar morphology (~100-250m) is superimposed on an alongshore variation consistent with the scale of the transverse ridges (~1000m). From the outer bar to the shoreline, and as the bar migrates landward, the variation becomes increasingly dominated by the rip-scale variation.

Hotspots of rip current activity were found consistently between years at Fort Pickens Gate, San Souci, Holiday Inn, Casino Beach, Avenida 18 and Portofino, as clusters of rip-scale variation.

ACKNOWLEDGEMENTS

First, I would like to thank my committee chair, Dr. Chris Houser, for all of his guidance, support and encouragement throughout my undergraduate and graduate research. It was the enthusiasm you showed in my geomorphology class that convinced me that this geomorphology stuff is pretty cool.

Thank you to my committee members, Dr. Doug Sherman, Dr. Steven Quiring, and Dr. Rick Giardino, for their guidance and support throughout the course of this research. Thank you for your guidance and support in my research. Your challenging, yet thought provoking, classes added immensely to my graduate school experience.

I would like to acknowledge and thank Aslak Grinstead for the use of his Matlab wavelet coherence package for this study, without there would have been much fewer pages and much more hair pulling.

Thank you to my friends and colleagues and the department faculty and staff for making my time at Texas A&M University a great experience. I will sincerely miss the experiences I've had with you guys in the field, in the department, and on the softball field.

Last and most importantly, a huge thank you to my parents, Ray and Sharn, for their encouragement, guidance (even if I didn't always follow it the first time around), and unconditional support. To my fiancé Kevin, I'm sure you know more than you ever wanted to know about rip currents. Thank you for acting like they're cool.

NOMENCLATURE

COI	Cone of Influence
CWT	Continuous Wavelet Transform
LBT	Longshore Bar-Trough Beach State
LTT	Low-tide Terrace Beach State
NWS	National Weather Service
RBB	Rhythmic Bar Beach State
SRIA	Santa Rosa Island Authority
TBR	Transverse Bar-Rip Beach State

TABLE OF CONTENTS

LIST OF FIGURES

FIGURE Page

FIGURE Page

LIST OF TABLES

CHAPTER I

INTRODUCTION

1.1 Study Purpose

The purpose of this study is to quantify the alongshore variation in nearshore bar morphology at Pensacola Beach, Florida to determine when the rip current hazard is at its greatest during the bar cycle. Specifically, the data will be used to identify hotspots of accretional rip channels and related to specific stages in the bar cycle. Recent studies hypothesize that the rip currents at Pensacola Beach are dependent on the migration of the bars and recovery of the beachface following an extreme storm capable of forcing the outermost bar offshore (Houser et al., 2011). Because there has not been a study of nearshore bar behavior along Santa Rosa Island (with the notable exception of Sonu (1972), who first described the morphodynamics of a transverse rip and shoal feature nearby), this remains an untested hypothesis. In this regard, the significance of this study is that it will assess nearshore bar migration patterns and determine under what morphological conditions lifeguards should be aware of that have historically caused an increase in rip current activity.

This thesis follows the style of Geomorphology.

1.2 Geologic Setting

The focus of this study is a 5.5 mile stretch of Pensacola Beach located on Santa Rosa Island in northwest Florida (Fig. 1.1). This low-lying barrier island is the second longest in the Gulf of Mexico and is seaward of a pre-Holocene barrier in Escambia Bay (Houser et al., 2008). Santa Rosa Island is a narrow, late Holocene barrier island that runs ~50 miles from its diversion from the mainland from East Pass in Choctawhatchee Bay at its easternmost point to Pensacola Pass at its westernmost point. This island has been impacted by a series of strong storms over the past decade causing overwash and breaching alongshore as well as shoreline retreat (Houser et al., 2008; Houser and Hamilton, 2009) including Hurricane Ivan in 2004, and Hurricane Dennis, Katrina and Tropical Storms Cindy and Arlene in 2005. Most recently in August 2010, tropical depression 5 made landfall in this area of northwest Florida, forcing bar 1 (the bar closest to the shoreline) to detach from the shoreface and migrate offshore.

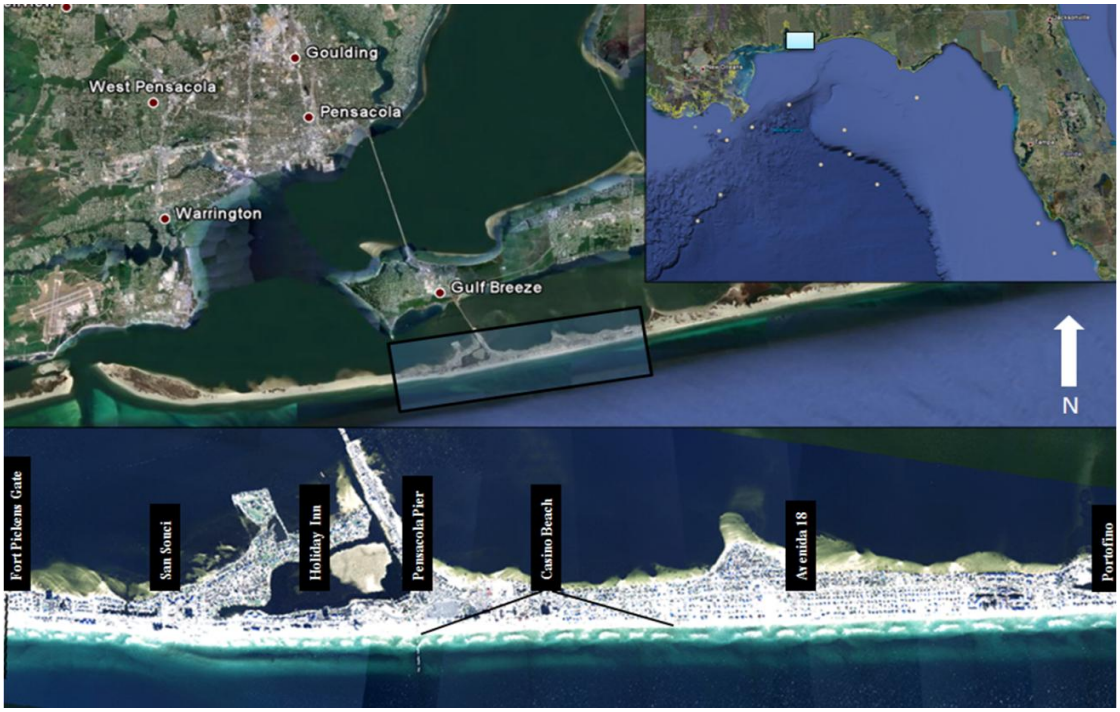

Fig. 1.1. Satellite image of study site location in reference to Florida (top right), Santa Rosa Island (top), and the stretch of coast being evaluated with wavelet analysis in this study (bottom). Landmarks are labeled in vertical text.

It has been hypothesized that the impact of these extreme storms and the behavior of the nearshore bar system is controlled by the geologic framework of the island (Houser et al., 2008). Specifically, there are a series of transverse ridges that sit on the inner continental shelf running southeast to northwest at an angle of 65° to the shoreline. The ridges are ~3m in height from crest to trough and extend from the shoreface to a depth of 15m. During storm events, these ridges focus waves toward the crests and defocus waves within the swales to create an alongshore variation in wave height. Little is known about how these ridges originally formed, but these specific ridges have been mentioned in several studies in this region of Florida (Hyne and Goodell, 1967). Despite their uncertain genesis, it has been shown that the shoreline-

transverse ridges force an alongshore variation in beach-dune morphology, washover penetration and the cuspate headlands along the backbarrier shoreline (Houser et al., 2008). Specifically, the transverse ridge crests are directly seaward of the largest foredunes backed by secondary dunes (backbarrier dunes and maritime forest), whereas the swales are seaward of the smallest dunes and a reflective beachface. Based on Fig. 1.2, it appears that the transverse ridges also force an alongshore variation in the nearshore bar morphology. Wave focusing at the ridge crests forces the outermost bar offshore, whereas wave defocusing within the swales creates smaller wave heights that allows the bar to be further landward.

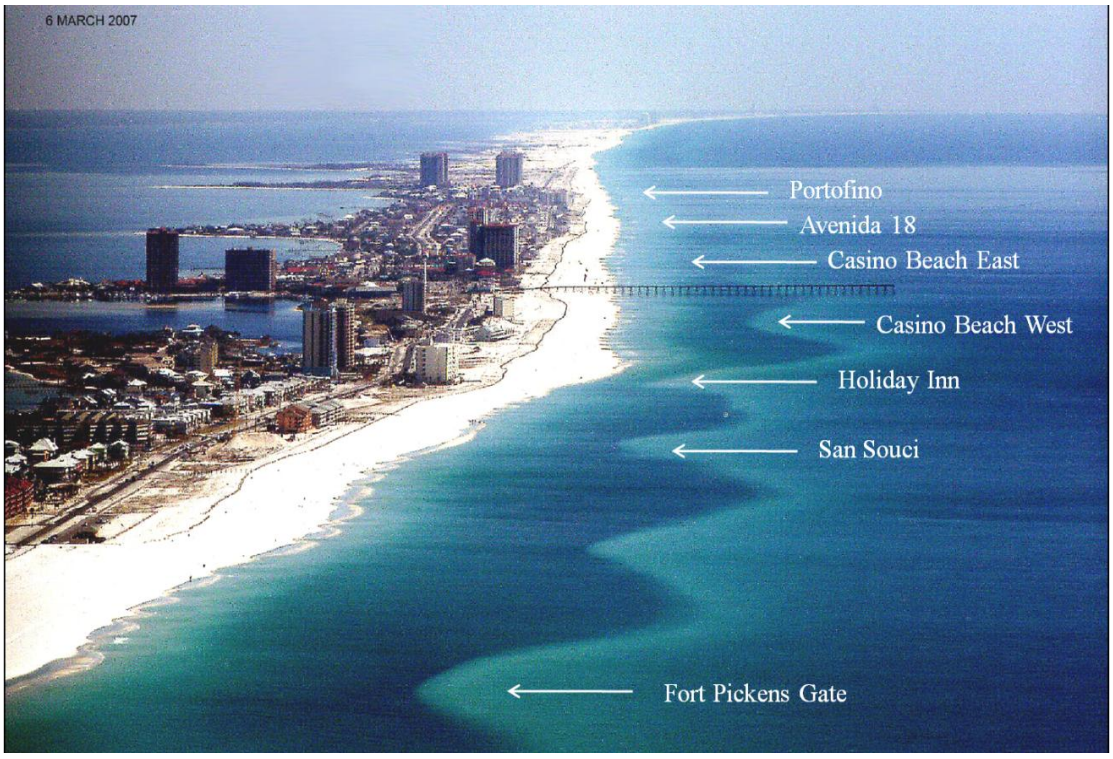

Fig. 1.2. Oblique image of Pensacola Beach. Locations of clustered rip current drownings from 2000 to 2009 are identified in white text. Image taken on March 6th, 2007 by Al Browder.

From 2000 to 2009, rip current drownings along Pensacola Beach were clustered between transverse ridges (Houser et al., 2008) and specifically at the landmarks shown in Fig. 1.2 The alongshore pattern in beach drownings implies that hotspots of rip current activity occur alongshore and are related to the location of transverse bars on the inner continental shelf. Drownings were also clustered in the years following an extreme storm impact (2000 to 2003 and 2005 to 2008), which suggests that the rip current hazard along Pensacola Beach is not uniform in time or space. This understanding is biased, as the drowning statistics collected by the Santa Rosa Island Authority are only recorded since 2000. The drowning statistics used in a recent, intensive study utilized records from 2004 to 2009 (Houser et al., 2011). While these drowning statistics identify times during which rip currents are present, the presence of rip currents does not necessarily mean a drowning will occur. Beach-users put themselves in danger each time they enter the water with or without the presence of rip currents.

The sinuous morphology of the outermost bar can be seen in Fig. 1.2; however, it is at the inner bar (bar 1) as it partial welds to the shoreline creating a tranverse bar and rip morphology that rip current related drownings occur. Fig. 1.3a shows a time-lapse image of Casino Beach from a camera mounted on a hotel in October of 2010. By time-lapsing the image over several minutes, the rip channels are highlighted as the troughs between bars with darker coloring because they are areas of little wave breaking. Areas in the surf zone with beige or white coloring are areas of wave breaking and constitute areas of shallower depth and therefore, a nearshore bar. Fig. 1.3a shows a typical transverse bar and rip state at Pensacola Beach. Rip channels are densely distributed

alongshore, and rip channels can be perpendicular to the shoreline but more commonly are oriented at more acute angles to the shoreline. On October 30th, 2010, there were as many nine or more rip channels present along this 0.7 mile stretch of Casino Beach. However, a transverse bar and rip morphology is not always present at Pensacola Beach. Only six weeks earlier, a rhythmic bar and beach morphology with a crescentic bar is seen in Fig. 1.3b. Understanding this dynamic morphology is an important step to identifying where along the shoreline and at what stage in the bar cycle are the greatest number of rip currents present.

Fig. 1.3. A time-lapse image taken from camera mounted on top of hotel overlooking Casino Beach shows (A) transverse bar and rip morphology on October 30th, 2010 and (B) a rhythmic bar-beach morphology on September 14th, 2010.

Fig. 1.3 continued**.**

1.3 Research Objectives

This research will examine at the multi-decadal variation in nearshore morphology at Pensacola Beach to determine at what points in the bar cycle and at what points alongshore do the greatest number of rip currents occur.

The specific objectives of this study were:

1. Quantify the alongshore variation in nearshore bar morphology through wavelet analysis from aerial photographs and satellite imagery from 1951 to 2004, and
2. To identify times of the bar cycle during which hotspots in rip current activity and the greatest number of rips take place.

1.4 Rip Current Formation

Rip currents are narrow, seaward-directed channels of water that persist from the shoreline out to or past the line of breaking waves in the surf zone (Shepard and Inman, 1950; McKenzie, 1958; Bowen, 1969). Rip current circulation is initiated as incident waves shoal on nearshore bars creating wave set-up landward of the breaking zone. This creates a longshore pressure gradient that generates a wave-induced momentum flux that funnels water through breaks or low points in the nearshore bars, also termed radiation stress (Longuet-Higgins and Stewart, 1964). The longshore radiation stress gradient results from an alongshore variation in wave breaking resulting from the presence of three-dimensional bars (Sonu, 1972; Wright et al., 1979; Wright and Short, 1984; Aagaard et al., 1997) or alongshore variability in the incident wave field (Bowen, 1969). It is generally believed that rip currents are topographically forced by complex bar morphology and have a form similar to the one shown in Fig. 1.3a (Sonu, 1972).

Rip currents may be broken structurally into feeder currents, the rip neck and the rip head. The feeder currents converge to create a rip current at the rip neck where the flow is directed offshore, as it flows between the breaks in nearshore bars. This is the most dangerous section of a rip current for swimmers as they can swim into the rip neck unknowingly and tire themselves trying to fight the faster moving currents, as they are pulled further away from the shoreline. As the velocity of the water being transported slows, a rip head forms, which is generally identified as a cloud of vortices seaward of the breaking waves. The rip neck may be between 10 and 30 m in width and is the fastest moving section of a rip current reaching velocities of 2 m/s (Sonu, 1972). Rip current

velocities are more commonly between 0.3 and 0.7 m/s (Sonu, 1972; Huntley et al., 1988; Short and Hogan, 1994). In general, rip current velocities vary with the tide with greater velocities found at low tide and lower velocities found at high tide in response to changes in wave energy dissipation (Aagaard et al., 1997; Brander, 1999; Brander and Short, 2000). Wave groups have been shown to create pulses in velocities through time (Shepard and Inman, 1950; Sonu, 1972; Brander and Short, 2001; MacMahan et al., 2004) due in part to infragravity waves.

1.5 Rip Morphology and Classification

Depending on the local beach morphology, rip currents have an alongshore spacing of between 100 and 1000m (Huntley and Short, 1992). This spacing is determined primarily by breaker height, sediment fall velocity and the surf zone width. Overall, linear and nonlinear morphodynamic models have produced rip spacing on average of 100 m, but studies range from 60m spacing (Sonu, 1972) to 500m (Brander, 1999) depending on the relative wave climate, although models to determine the mechanism driving rip spacing have not been successful (MacMahan, 2005).

Recently, self-organization has been proposed as the dominant hypothesis for rip current forcing alongshore (Deigaard et al., 1999; Coco and Murray, 2007) over the previous hypothesis of alongshore standing waves (Bowen and Inman, 1969). The dominant variable believed to effect self-organization is wave height, but this has not been compellingly supported in the literature (Short, 1985; Huntley and Short, 1992; Lafon et al., 2005). Nonlinear self-organization models (Damgaard et al., 2002; Coco et

al., 2001; Reniers et al., 2004) suggest that crescentic bar spacing is proportional to the width of the surfzone (Coco and Murray, 2007), contradictory to field studies, which show a quasi-rhythmic spacing alongshore that is not tied to the width of the surfzone (Huntley and Short, 1992; van Enckevort et al., 2004; Holman et al., 2006).

Other variables have been suggested (see Greenwood and Davidson-Arnott, 1979) as being proportional to crescentic bar spacing including the surrounding bathymetry (Calvete et al., 2007), migration rates combined with wave energy flux (Ruessink et al., 2001; van Enckevort and Ruessink, 2003; Holman et al., 2006), the area of the trough that transports feeder currents for the rip current (Deigaard et al., 1999), the width of the bar crest to the shoreline (Hino, 1974; Deigaard et al., 1999; Damgaard et al., 2002) or the depth at the bar crest (Calvete et al., 2007).

There have been several attempts to classify rip currents and their respective beach environments visually (Short, 1985) or by quantitative methods (Short and Brander, 1999). Summarized in Table 1.1, the most widely used system of classification was created by Short (1985), which categorizes rip currents into three groups: mega rips, accretional rips and erosional rips. Accretional rip currents are stationary, can persist for days to weeks, and are topographically forced by prominent bars and rip channels. Erosional bars migrate alongshore and persist from minutes to days. Mega rips are also topographically controlled and can persist from hours to days and are most common on embayed beaches (Short, 1985).

Table 1.1.
Table of rip current classifications. Modified from Short (1985).

Rip Type	Spatial Persistence	Temporal Persistence	Morphology	Dynamics
Accretional	Stationary	Days to Weeks	Prominent rip channels and bars	Edge wave controlled; Topographically forced; Infragravity pulses
Erosional	Merging and longshore migration	Minutes to Days	Ephemeral until migration ceases	Edge wave controlled; Infragravity pulses
Mega	Stationary; Controlled by shoreline morphology and / or by nearshore topography	Hours to Days	Well developed rip channel	Infragravity pulses and topographic effects

Whereas rips can develop on any beach during storm conditions (Short, 1985), intermediate beach morphologies are the most common beach type in which rip currents as a result of their rhythmic topography and resulting surf-zone circulation (Wright and Short, 1984). According to Short's classifications (Table 1.1) and the example of rip current pattern shown in Fig. 1.4, the rip currents along Santa Rosa Island are accretional rips as a result of their topographically forced morphology, temporal persistence between days to weeks, and their stationary location. More specifically, they are defined by Santa Rosa Island's transverse bar and rip beach state due to the presence of rip channels and bars. These beach environments can create strong rip currents under weak surf conditions, which presents an even greater hazard to swimmers. It is the persistence of these accretional rip currents at Pensacola Beach that have created a hazard for beach users, making it the most hazardous beach in the United States for beach drowning by rip currents in 2002.

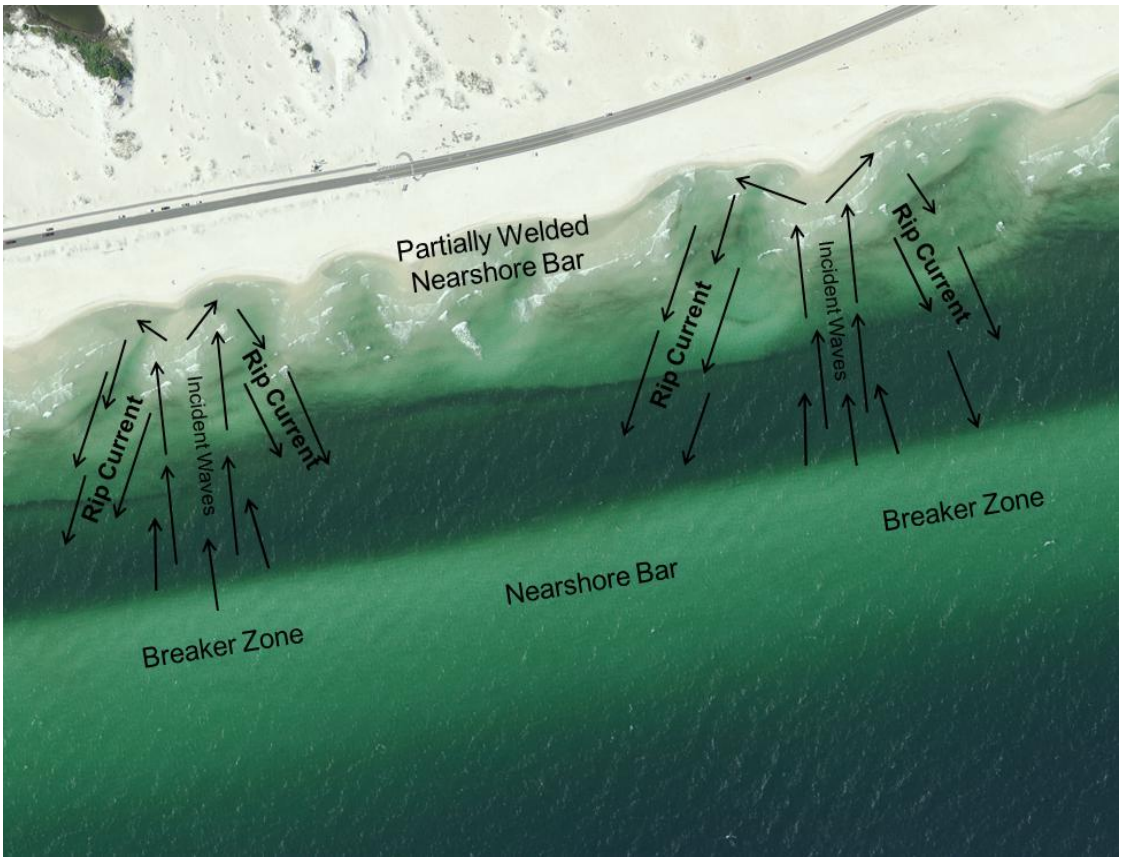

Fig. 1.4. Diagram of rip current pattern at Pensacola Beach on 3-dimensional partially welded bar.

1.6 Role of Nearshore Bar Dynamics

Nearshore bars migrate offshore in response to, and onshore in recovery from extreme storms. Migration offshore is caused by breaking waves impacting the bar crest which creates an offshore-directed current also known as undertow (Ruessink et al., 1998; Plant et al., 2001). Onshore bar migration is caused by skewed incident waves which transport sediment landward causing the bar to migrate in the landward direction. The morphology and migration of nearshore bars affect circulation and transport of sediment in the nearshore. As a result, the timing and location of rip channels is

dependent on the evolution of the nearshore bars that are typically oriented parallel to the shoreline and are important for sediment transport between the beach and shoreface. Specifically, it is the migration of nearshore bars through the bar cycle (see Fig 1.5) in response to extreme storms that drives rip channel formation.

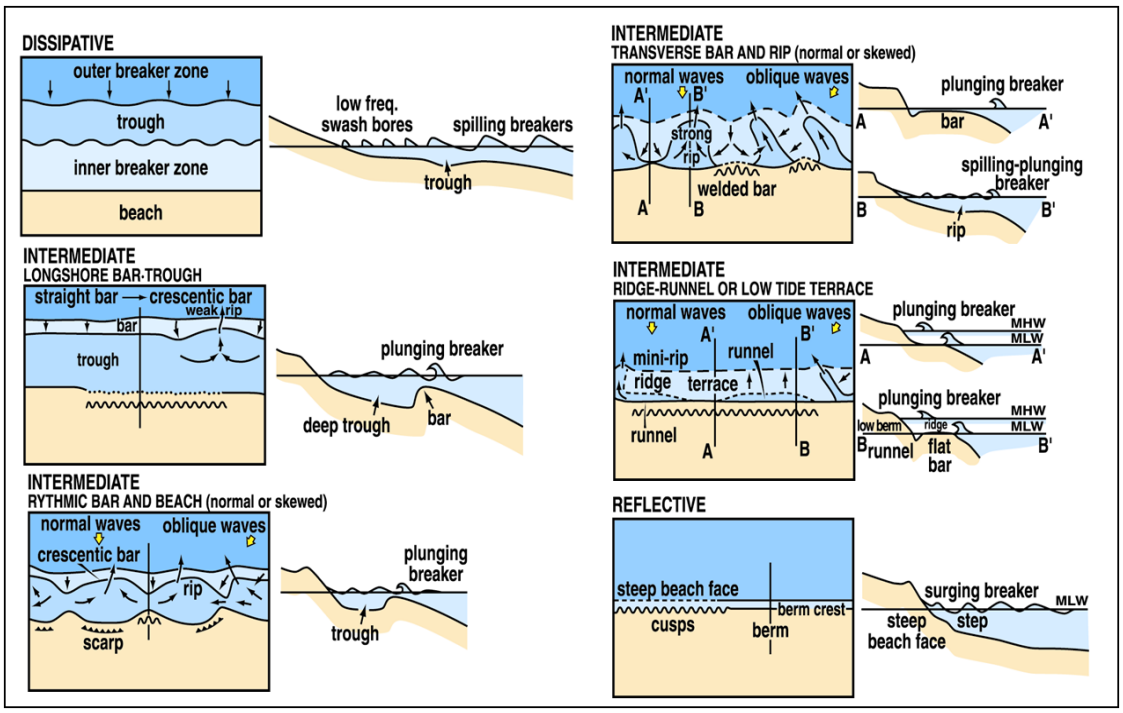

Fig. 1.5. Configuration of the six major beach types. Modified from Wright and Short (1984).

The beach morphodynamic states that categorize nearshore bar migration stages are defined by the surf scaling parameter (Guza and Inman, 1975):

$$\epsilon = a_b\omega^2/(g\tan^2\beta), \quad (1)$$

where a_b is the breaker amplitude, ω is the radian frequency of indicent waves ($2\pi/T$ where T is the period), and g is the acceleration resulting from gravity and β is the gradient of the beach. A beach is considered dissipative if $\epsilon > 20$ and reflective if $\epsilon < 2.5$. Anything located between these values is considered to be an intermediate beach state with smaller ϵ values corresponding to more reflective and larger ϵ values to a more dissipative state. The intermediate beach states (see Fig. 1.5) are broken down further into four categories: Longshore bar-trough, rhythmic bar and beach, transverse bar and rip, and low-tide terrace.

A longshore bar-trough (LBT) morphology is characterized by a straight or crescentic nearshore bar with a trough on its landward edge and a shoreline that may be straight or have cusps. The rhythmic bar and beach (RBB) morphology presents a crescentic bar with horns migrating more landward and aligning with mega cusp horns alongshore. Rip currents may form at the bay sections of the crescentic bar. The transverse bar and rip state (TBR) develops during an accretionary sequence when the horns of the crescentic bar welds with the horns of the beachface. Rip currents are created when water flows seaward through the topographic channels created from the partial welding of the nearshore bar (Sonu, 1972; Wright and Short, 1984) producing the strongest rip current circulation. The cusped shoreline of the RBB beach state is softened by the partial welding of the bars and creates a more undulating shoreline profile. The low tide terrace or ridge and runnel beach state (LTT) is formed as the bar welds almost entirely onto the beachface creating a terrace at low tide. Small rip currents may be present during this stage but are more dominant during the TBR and RBB beach states.

A beach may progress through these beach states assuming a period of low-energy conditions. At any stage, a reset event will detach the nearshore bar and migrate offshore, reverting the beach back to a longshore bar and trough morphology and restarting the bar cycle. Areas experiencing episodic storm impacts experience a repeating bar cycle with bars migrating offshore during storm response and migrating landward during storm recovery. Extended periods with low-wave activity lead to onshore bar migration and a full progression through the bar cycle from LBT to RBB to TBR to LTT. A series of closely spaced storms would stimulate continued offshore bar migration which would lead to bar decay at the outer margin of the surf zone between 900m and 1300m offshore (Ruessink and Kroon, 1994; Aagaard et al., 2010).

In general, nearshore bars migrate onshore during calm conditions and offshore during high-energy conditions (Shepard, 1950; Komar, 1976). A strong correlation has been shown between bed return flow and offshore bar migration in high energy conditions (Thornton et al., 1996; Aagaard et al., 1998; Gallagher et al., 1998). During this process, sediment from an existing bar is suspended by breaking waves and transported offshore by bed return flow which forces offshore bar migration to the outer margin of the surf zone. During periods of calm conditions, bars migrate onshore because of oscillatory velocity skewness under weaker wave conditions (Hsu et al., 2006). This velocity skewness is attributed to the change in wave shape as it enters shallow water, shoals and forces water in the landward direction, therefore increasing its forward velocity (Stive, 1986). This nearshore bar migration pattern is due in part to a net offshore migration of sediment in the cross-shore direction (Ruessink et al., 1998;

Plant et al., 2001). This positive feedback increases the wave energy dissipated on the inner bar creating greater wave set-up (Longuet-Higgins and Stewart, 1964) and therefore an increased offshore transport rate that cause the next nearshore bar in the sequence to migrate offshore at an increased rate (Wijnberg, 1997).

Bars come in many forms and can have a linear, straight form that is typically consistent with offshore migration whereas a more three dimensional sinuous morphologies are associated with onshore migration and bar attachment to the shoreline (Wright and Short, 1984; Birkemeier and Holland, 2001). Crescentic bar morphologies, which have been called lunate bars (Shepard, 1952) are more complex bar systems that have not been examined in as much detail as linear bars because of their added 3-dimensional complexity. These features can be described as a series of horns of crescentic bars that weld onto the shoreface. These features are more common in microtidal environments, such as Pensacola Beach and are believed to be strongly influenced by alongshore currents as they have been shown to migrate with the prevailing wave direction (Ruessink et al., 2000; van Enckevort and Ruessink, 2003). As previously noted, crescentic bars represents a bar in a state of recovery as a straight, linear bar migrates landward, partially welding with the shore, creating an alternating alongshore pattern of horns and bays which otherwise serve as rip channels. If calm conditions continue, the bar will continue to attach to the shore and rip channels will disappear (Ruessink and Kroon, 1994; Houser and Greenwood, 2005; Aagaard et al., 2004). The presence of crescentic bars categorizes a beach as being in a transverse bar rip state under the Wright and Short (1984) beach state model. As the bar welds to the

shore, the beach state changes to a low tide terrace morphology (Wright and Short, 1984). Alternatively, if high energy conditions are introduced, the bar will detach from the shoreline and become more parallel in form, quickly reverting back to a linear bar morphology. Rip currents develop as a bar migrates landward and partially welds to the shoreline at discrete points alongshore (RBB) or along the length of the coastline as the entire bar becomes partially welded (TBR). If a reset event occurs, the bar will migrate offshore and rip channel formations will be lost until the bar migrates landward again, restarting the sequence of stages in the bar cycle.

Recent studies have suggested that nearshore bar morphology may be further modulated by the morphodynamics of an outer bar within the system (Ruessink and Terwindt, 2000; Aarninkhof et al., 1998; Masselink, 2004). This potential feedback, also known as bar coupling, is most easily analyzed in micro-tidal environments because smaller tidal variations limit the variation in mean water depth, which can change the relationship between wave breaking and refraction (Castelle et al., 2010).

Castelle et al. (2010) in the first nearshore model to analyze double bar coupling, showed that nearshore bar coupling was caused by wave refraction and depth-induced breaking over the outer bar which creates an alongshore variation in horizontal circulation. This indicates that the inner bar morphology is largely driven by the outer bar morphology (Houser and Greenwood, 2005). A smaller alongshore wavelength in the outer bar creates more wave focusing by refraction, which has a greater effect on the inner bar morphology and creates an in-phase coupling morphology. If wave breaking is

too great and overcomes the wave focusing, out-of-phase or 180° coupling of bars emerges (Castelle et al., 2010).

This out-of-phase bar coupling was seen in studies on wave-dominated shorelines between an inner and outer bar (van Enckevort and Wijnberg, 1999; Castelle et al., 2007; Sonu, 1973; Haas et al., 2003). Following a storm event, inner and outer bar variability has been shown to develop independently of one another and become coupled over time (Ruessink et al., 2006; Castelle et al., 2010). Ruessink et al. (2007) showed the transformation of a non-coupled to coupled system as calm conditions prevailed and the outer bar migrated landward creating a more variable alongshore morphology. As this migration initiated, the inner bar morphology became coupled to the outer bar morphology because of the alongshore variability of wave height and wave focusing from the outer bar morphology.

Bar coupling is a morphodynamic feedback that would be most easily be examined using decadal variations in nearshore bar migration and morphology. Analyzing these potential mechanisms at longer time scales is important to try and extract possible patterns in behavior, which is true for all nearshore bar dynamics. A decadal time scale may include multiple extreme storm events and the migration of nearshore bars as a result of the response to and recovery from these extreme storm impacts. Evaluating a beach over a decadal scale allows spatial and temporal patterns in rip spacing or location to become clear if they are present. Noticing the timing of the rip current hazard in response to storms is an important tool to deciphering periods of strong rip current hazard in the future. In addition, analyzing the timing and location of past rip

current hazards within the bar cycle is an important factor in predicting the rip current hazard in the future.

1.7 Rip Current Hazard / Safety at Pensacola Beach

Rip currents account for 80% of all rescues and assists by Florida lifeguards and are considered to be the leading natural disaster within the state (Lushine, 1991; Lascody, 1998). Rip currents downings range from 100 to 150 a year in the United States (Fletemeyer and Leatherman, 2010). It is because of the rip current hazard that coastal management issues have become an increasing area of concern (Short and Hogan, 1994; James, 2000; Jimenez et al., 2007; Turner and Anderson, 2007). Whereas rip current drownings are more commonly associated with high-energy coasts such as the east coast of Florida, Pensacola Beach was named as the most hazardous beach in the United States for beach drownings as a result of the persistence of the rip channels and the relatively large number of drownings (The Tuscaloosa News, 2002). The Santa Rosa Island Authority (SRIA) estimates that 90% of the 401 rescues in 2010 are the result of beach users getting caught in rip currents.

In 2002, state legislation in Florida required a uniform beach safety program be established that require public beaches and coastal areas to display warning and beach safety flags. An amendment to this section in 2005, required beach warning flags to become standardized to the system that is used currently. The standardized warning flag system is shown in Fig. 1.6 along with the standard rip current sign posted at beach access points around the country. Despite these efforts, there were 4 drownings at

Pensacola Beach between 2004 and 2010 and there have already been 2 drownings in the spring of 2011. Warning signs are required at all beaches in Florida and are posted at every beach access point along Pensacola Beach, regardless of if they are located where lifeguards are stationed. The rip current warning sign generalizes rip currents into a simplified form that they rarely resemble and as a result it has been suggested that rip current warning methods be re-evaluated (Fletemeyer and Leatherman, 2010).

Fig. 1.6. On the left, the standardized beach warning flag sign. On the right, the standard rip current sign used along the Gulf & East Coast. Both signs are posted at all beach access points along Santa Rosa Island. Images obtained from NOAA.

As previously noted, rip current drownings from 2000 to 2009 were clustered in locations between transverse ridges (Houser et al., 2011). This trend in beach drowning implies that hotspots of rip current activity do occur alongshore and are directly related to the location of transverse bars on the inner continental shelf. These hotspots of rip

current activity are patrolled by lifeguards posted along Pensacola Beach who have run 2425 rip current related rescues since 2003. Lifeguards are posted from March to October along Casino Beach in lifeguard stands. Lifeguards are posted at two additional locations along Pensacola Beach at Park East and Fort Pickens Gate from May to August each year. The signs (see Fig 1.6) are posted at beach access points such as beach walkovers and parking lots along with the currently flying flag to inform the public about the current conditions.

Most parking lots and building on Santa Rosa Island were originally planned and built in areas between dunes and in areas with smaller dunes in order to keep the natural dune structure of the island intact. Areas that correspond with smaller dune heights were also correlated with transverse ridge troughs which represent areas of a greater sloping beach face as well as wave defocusing (Houser et al., 2008). These areas have been shown to correspond with accretional rip current activity and are the primary sites of recent drownings (Houser et al., 2011). These hot spots in rip current activity become a concern when evaluated with coastal management studies that find most beach-users occupy an area within 100-250m from main beach access points with the maximum number of beach-users around 150m (Jimenez et al., 2007). Rip current drowning at Pensacola Beach have been shown to be clustered alongshore in conjunction with the troughs between transverse ridges (Houser et al., 2011). From west to east these five clustered areas alongshore include Fort Pickens Gate, San Souci, the Holiday Inn, Casino Beach and Portofino (see Figs. 1.1 and 1.2).

Decisions about the rip current hazard are dependent on the daily surf zone forecasts provided by the National Weather Service (NWS), which is based on studies by Lushine (1991a, b). These rip current outlooks are based on the wind and / or wave conditions forecast for that day and whether or not they are expected to support the development of rip currents. Meteorological factors have also shown to have an influence on rip current intensity as 90% of rip current drowning and rescues in two Florida counties took place when wind speeds were 12 m/s or greater, directed onshore and within 30° of normal (Lushine, 1991a, b). Rip current warnings and the decision regarding which beach safety flag to fly at any given time are dependent on the NWS rip current forecast. This system has recently been criticized for not including beach-user statistics, which vary depending on the time of year, the day of the week, and in the event of a holiday as well as on meteorological factors such as precipitation or cloud cover (Gensini and Ashley, 2010).

The current rip current warning system provided by the NWS also lacks an evaluation of the nearshore bar state at each of its rip current forecast locations. It is the movement of nearshore bars through the bar cycle that dictate when a rip channel is present. By better understanding at what points in the bar cycle rip channels form, rip current forecasting may become more accurate.

A comprehensive rip current forecasting system that includes weather, beach-user statistics and nearshore morphology would be a valuable tool for coastal managers. Unfortunately, a forecast based on these variables would have to be site specific and require constant monitoring of beach users and bar morphology. In the latter case,

lifeguards can alter patrols and stands based on the evolution of the bar morphology through the bar cycle to adapt to the changing position of the rip current hazard.

CHAPTER II

METHODOLOGY

2.1 Research Method Objectives

To meet the objectives of this study, aerial and satellite imagery were collected for the sections of Santa Rosa Island within Escambia County. The images were georeferenced and the shoreline, inner bar and outer bar were digitized. The data from these features were analyzed using wavelet analysis to identify rip current hotspots alongshore and to determine at what stage of the bar cycle do these develop along Pensacola Beach.

2.2 Aerial Photographs

Aerial images were obtained for Santa Rosa Island through the State of Florida and the United States Geological Society. Aerial photographs were collected based on public availability, continuous coverage of the western end of Santa Rosa Island and visibility of the shoreline, inner bar and outer bar (if present). Once all available images were collected, the boundaries of the final study area were chosen based on the following factors: 1) inclusion of San Souci, the Holiday Inn and the full extent of Casino Beach and Avenida 18 (the drowning hotspots), 2) extend as far east as possible while maintaining a relatively consistent spacing in imagery year, and 3) include Fort Pickens Gate or as close to Fort Pickens Gate as possible without excluding imagery years that have already been chosen. Based on these factors, the western boundary is

close to Fort Pickens Gate (87° 5’2.576” W 30° 20’28.361” N) and the eastern boundary is at Portofino (87° 10’34.135” W 30° 19’30.842” N). The images were georeferenced to a NAD 1983, UTM Zone 16N spatial reference using ArcGIS. Georeferencing these images into a UTM coordinate system allowed digitized data to be extracted in meters, which prevented a conversion from degrees, minutes, seconds for wavelet analysis. The georeferenced images are shown in Fig. 2.1 by year.

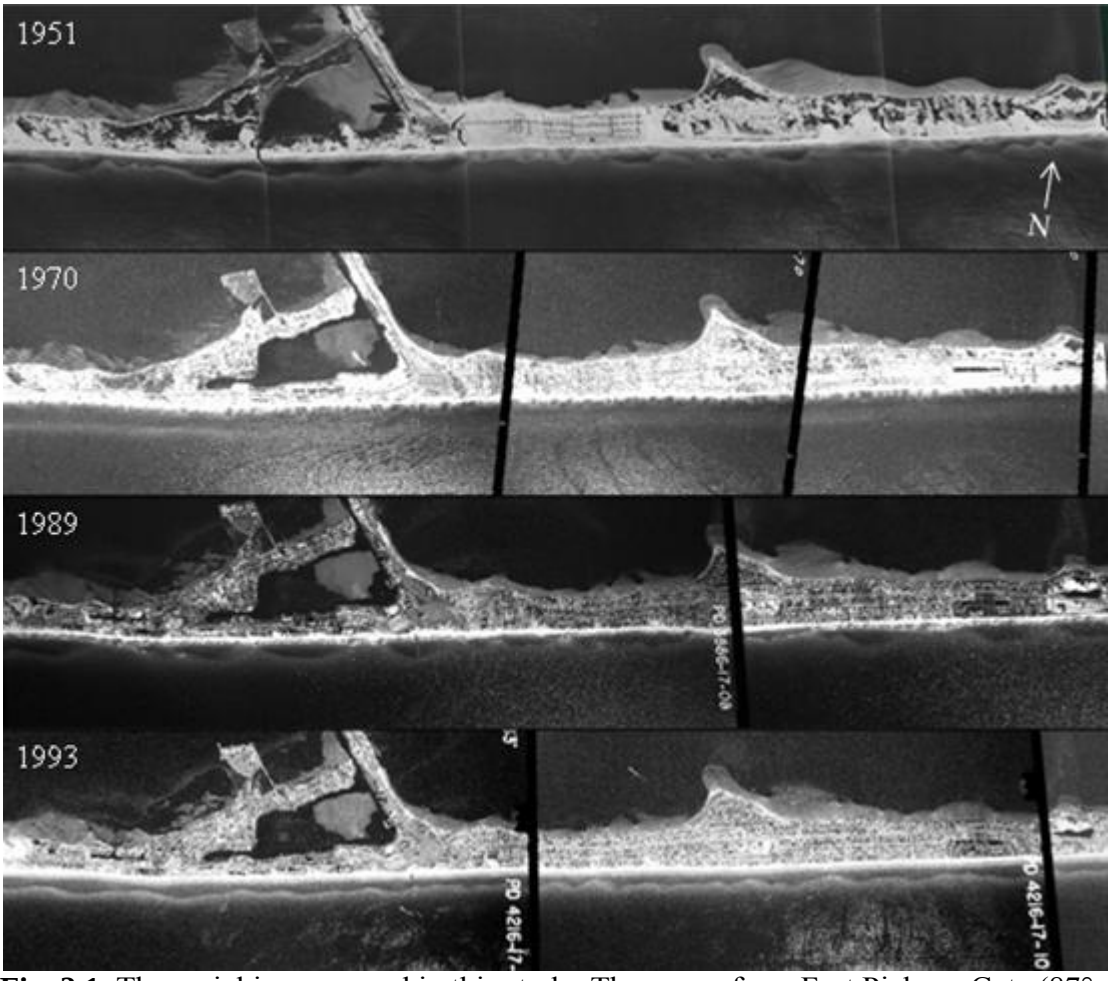

Fig. 2.1. The aerial images used in this study. They span from Fort Pickens Gate (87° 5’2.576” W 30° 20’28.361” N) in the west to Portofino (87° 10’34.135” W 30° 19’30.842” N) in the east.

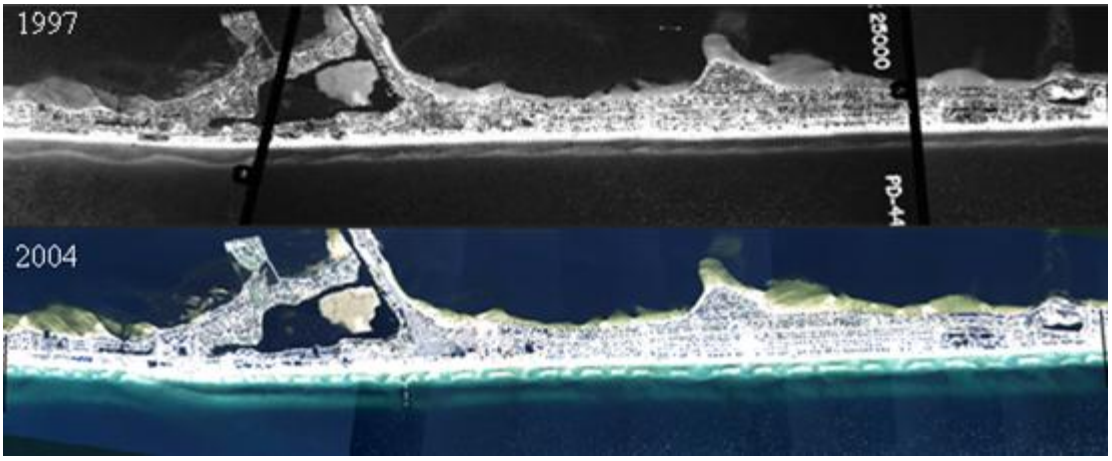

Fig. 2.1 continued.

As is further discussed in the Results section, the aerial images contain a number of diverse beach states. The nearshore bars range in number, distance from the shoreline, sinuosity, their degree of welding to the beachface, and in 2- and 3-dimensional morphology. The shorelines also vary in linearity and the presence of cusps and horns alongshore. The aerial photos shown in Fig. 2.1 were interpreted using the Wright and Short model for beach state classifications (1984). An example of the 4 intermediate beach state classifications as defined by Wright and Short (1984) can be seen in Fig. 2.2. This classification takes into consideration the shoreline and bar 1, so bar 2 in 2004 will not be included as a part of consideration for the beach state classifications. All years of aerial imagery will be assigned a beach state classification. For example, the imagery in the top right hand corner of Fig. 2.2 can be considered longshore bar-trough because it fits the description from Wright and Short (1984). It has a straight to crescentic nearshore bar with a distinct trough between it and the linear shoreline. Without using on-site observations and measurements, the aerial images can be classified by intermediate beach state and following the classification descriptions.

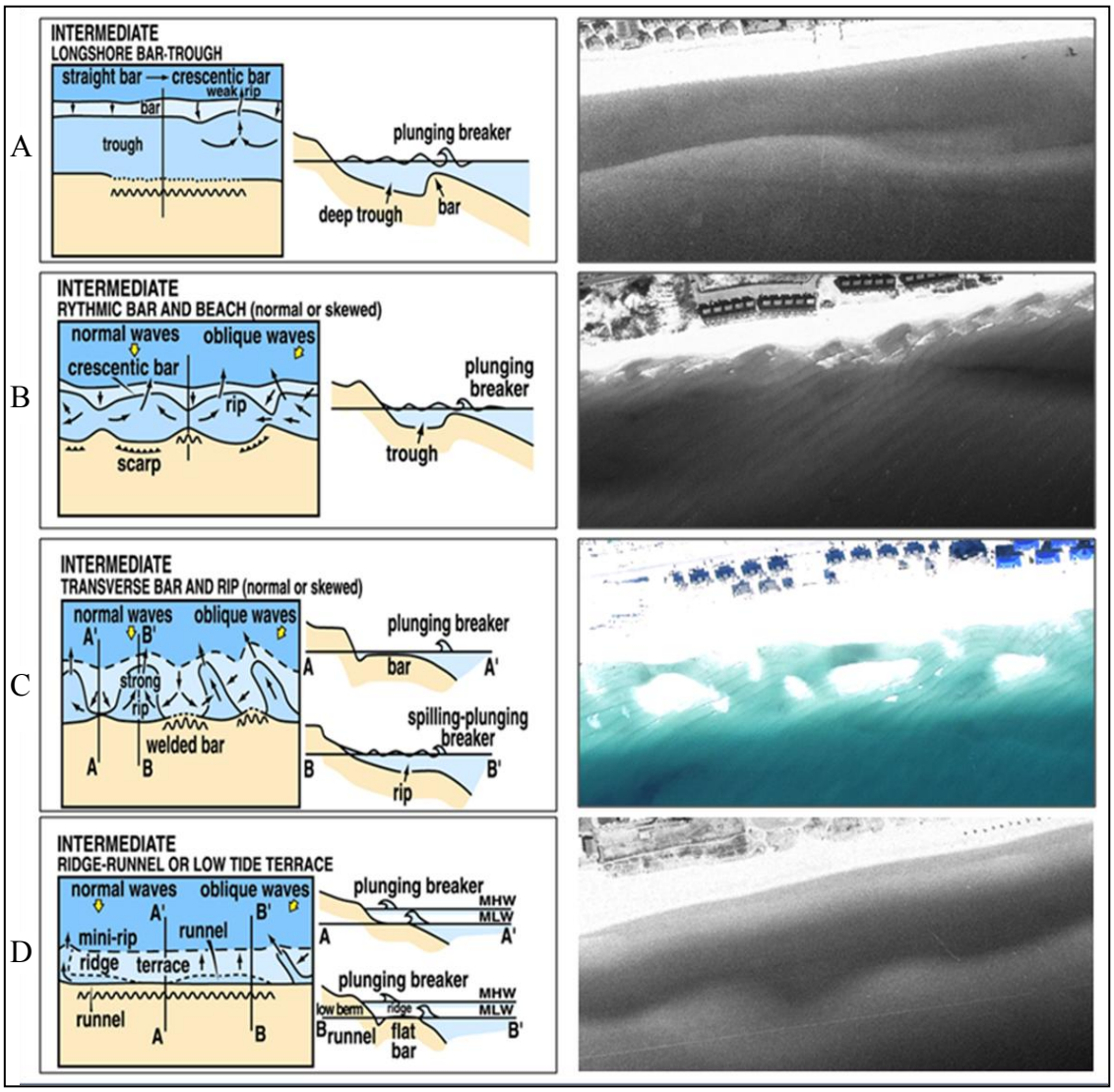

Fig. 2.2. Examples of intermediate beach states defined by Wright and Short (1984) (left) and representative photos of those beach states taken from aerial photos used in this study (right). Beach states are (A) longshore bar-trough, (B) rhythmic bar and beach, (C) transverse bar and rip and (D) low tide terrace.

2.3 Digitizing Nearshore Features

Nearshore features were digitized using ArcGIS for each year with aerial imagery. This was completed with the pencil tool in the Editor toolbar. The shoreline,

inner bar and outer bar were drawn digitally for all years (see Fig. 2.3). The landward edge of the bar was drawn for both the inner and outer bar. The shoreline was drawn at the middle of the swash zone, approximately. This was facilitated by the darker color of the swash zone in the aerial images. If channels dissected the features, the digitized line was drawn to most accurately capture the landward edge of the nearshore bar or middle of the swash zone along the shoreline. At the beginning of a channel, a straight line would be drawn in the direction of the closest point reconnecting the line to the nearshore bar or shoreline.

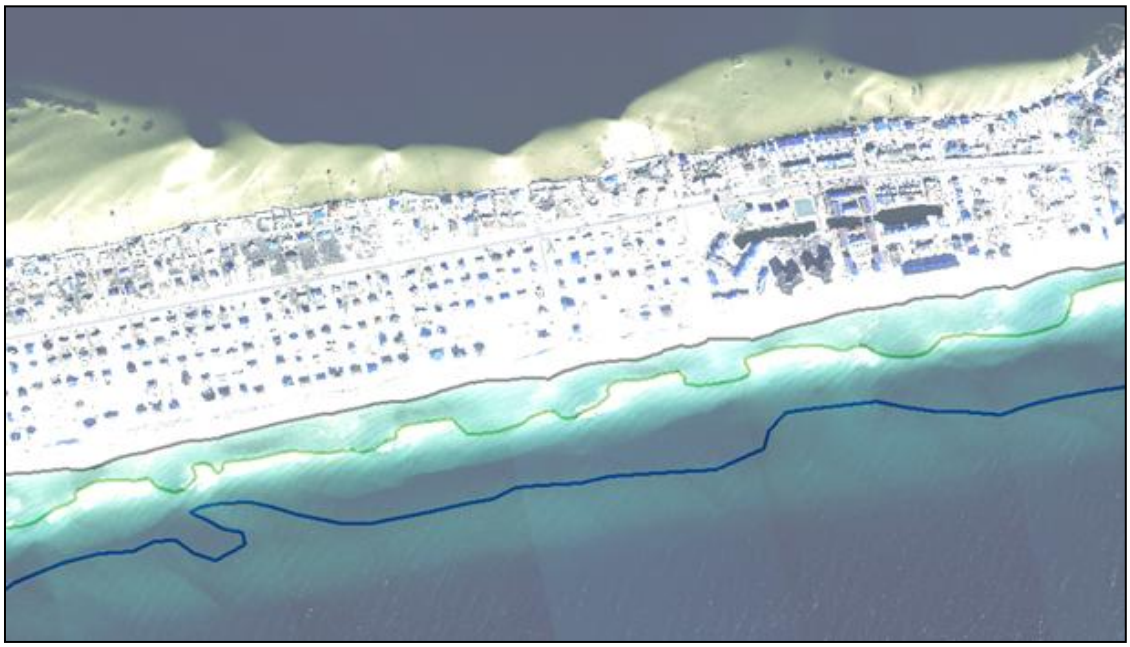

Fig. 2.3. Image from 2004 showing digitized forms of the shoreline (grey), inner bar (green) and outer bar (blue) created in ArcGIS.

The welded bar in 1993 and the partially welded bar in 1970 were digitized as a part of the shoreline. This presented less confusion when deciphering what was

considered the shoreline and bar 1. After the bars were digitized, they were assigned vertices based on points drawn to create the digitized line using the 'Feature Vertices to Points' tool in the Features toolset in the Data Management toolbox. XY coordinates were then assigned using the 'Add XY Coordinates' tool in the same toolbox. The features were detrended using Matlab to allow the data to be analyzed without the overlying trend of the slanted coastline and therefore remaining nearshore features. The data was interpolated at 10 meter spacing alongshore to prepare the data for wavelet analysis. Using MATLAB, the data sets for the nearshore features were standardized in space by removing the minimum value from each nearshore feature from the entire dataset for that feature. This step allowed shorelines, inner bars and outer bars to be directly compared, regardless of year or morphology. If any 'looping back' was present in the digitized features, it was removed by calculating the most direct route between points whereas keeping as much of the variation as possible.

2.4 Wavelet Analysis

Wavelet analysis is a valuable technique that has been utilized to analyze non-stationary data within the geosciences. Seafloor bathymetry (Bazartseren and Holz, 2002), foredune height (Houser and Mathew, 2011), ocean wind waves (Elsayed, 2010), turbulence scales for wind velocity (Jordan et al., 1997), and wave growth and breaking (Liu, 1994) are just some of the areas that this technique has been applied to within the coastal environment and geomorphologic studies.

Nearshore studies using wavelet analysis include analyzing beach oscillation and rotation patterns on a decadal scale (Short and Trembanis, 2004), variability of beach profiles (Li et al., 2005), foredune height alongshore (Houser and Mathew, 2011) and nearshore bar coupling (Coco et al., 2005; Ruessink et al., 2006). More specifically, Ruessink et al. (2006) used continuous wavelet transforms to look at the migration of the inner and outer bar and their variability alongshore. Wavelet analysis was a valuable technique for this study and other nearshore studies because it allows for the patterns and coherence of nearshore features to be evaluated alongshore.

First introduced by Grossman and Morlet (1985), wavelet analysis allows for a signal to be evaluated for amplitude and phase at each spectral component locally within the signal (Torrence and Compo, 1998). A wavelet allows data to be decomposed and localized in both frequency (scale) and time domains simultaneously. A wavelet transform leaves the higher frequency components of the signal intact which allows for a high resolution evaluation of the signal. This technique overcomes some shortcomings with other analysis methods including Fourier analysis which only allow the overall strength of the signal to be evaluated at certain predetermined frequencies. In addition, other techniques do not allow signal strength to be analyzed in conjunction with their location within the spatial or temporal series. Areas of statistical significance within the wavelet maps were introduced by Torrence and Compo (1998) and set at the 5% significance level for this study (Ruessink et al., 2006; Castelle et al., 2010).

The following are concepts relevant to my research and wavelet analysis. For a more detailed explanation, see Torrence and Compo (1998) and Farge (1992). The

wavelet transform is a convolution of a sequence x_n, where n = 0… N-1, with a translated and scaled version of a normalized wavelet function $\varphi_0(\eta)$:

$$W_n^x\ s\ =\ \sum_{n'=0}^{N-1} x_{n'} \psi^*\ \frac{n'-n\ dx}{s}\ , \tag{2}$$

where (*) indicates the complex conjugate, *dx* is the time step, N is the number of points in the time series, *s* is the width of the wavelet scale also known as dilution function and *b* is the time lag or translation parameter. The Morlet wavelet (see Fig. 2.4) is used in this study because the temporal and frequency domains are able to localize characteristics of the data set well (Torrance and Compo, 1998) and have successfully been used in previous research on nearshore bars (Ruessink et al., 2006; Castelle et al., 2010). The Morlet wavelet is defined as:

$$\psi_0\ \eta\ =\ \pi^{-1/4} e^{i\omega_0 \eta} e^{-\frac{1}{2}\eta^2}, \tag{3}$$

where η is the nondimensional time parameter and ω_0 is the nondimensional frequency (is 6 for the Morlet wavelet). A nonorthogonal wavelet function is used for the continuous wavelet transform (Farge, 1992) instead of the discrete wavelet transform because it is better equipped to extract features from the signal.

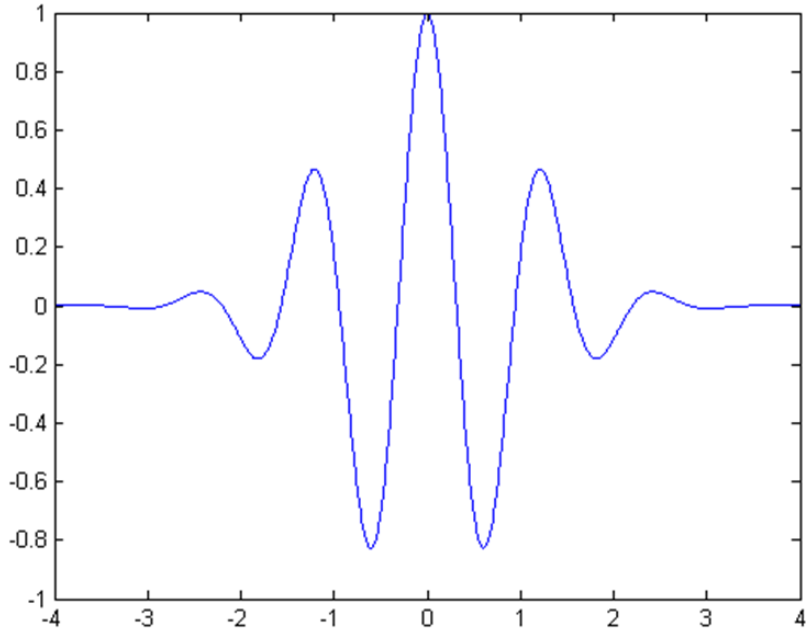

Fig. 2.4. The Morlet wavelet wave base.

The computations used in this paper were provided by A. Grinsted (http://www.pol.ac.uk/home/research/waveletcoherence/) and based on software developed by Torrence and Compo (http://paos.colorado.edu/research/wavelets/). An example of a wavelet map for a continuous wavelet transform can be seen in Fig. 2.5.

The cone of influence (COI) is the point at which edge effects can affect data integrity and this is the reason for the rounded cone shape at the bottom of the wavelet maps (Fig. 2.5). The COI is required because the transform assumes the data is cyclic, which produces errors at the beginning and end of the wavelet because these areas are not completely localized in time.

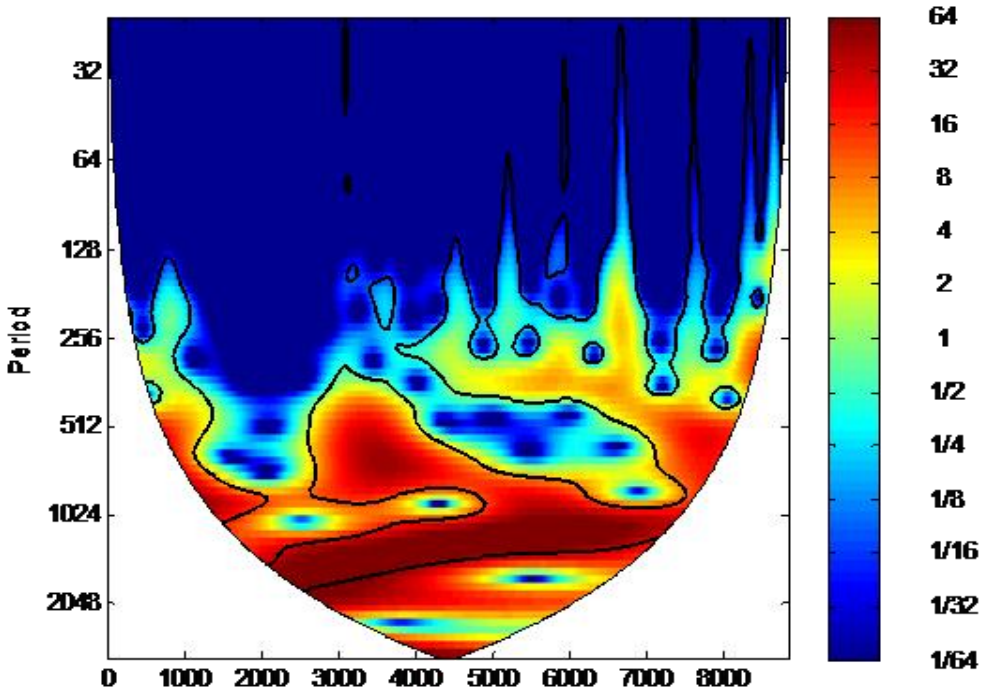

Fig. 2.5. An example of a continuous wavelet transform. Data is shown within the cone of influence (COI). The black lines indicate data exceeding the 95% confidence interval.

On the wavelet maps, relative power is designated by the color spectrum with higher relative power having warmer colors (red to yellow) and lower relative power having cooler coloring (turquoise to purple). Areas with a 95% confidence are surrounded in a bold black line which differentiates red noise from white noise. The confidence level was set by the user in the Matlab wavelet script for continuous wavelet transforms.

2.5 Global Wavelets

The global wavelet spectrum averages the sum all local wavelet spectra:

$$\overline{W}_n^2 \; s \; = \frac{1}{n_a} \; \sum_{n'=0}^{N-1} W_n(s) \; , \tag{5}$$

which has been shown to show the power spectrum of a time series with an impartial and consistent estimation. The detrended data for each shoreline, inner bar and outer bar for each year were used to global wavelet spectrums for each combination of years and coastal features. Global wavelet spectrums allow the more dominant frequencies in the data series to be emphasized. Often spikes in the signal at given frequencies can help to identify the underlying mechanisms driving the data variation. These were completed in the software AutoSignal.

CHAPTER III

RESULTS

3.1 Beach State Classification

The nearshore morphology along Santa Rosa Island was classified according to the beach state types of Wright and Short (1984), which were introduced in Fig. 1.4. The aerial images with their beach state classifications for each year are presented in Fig. 3.1. The aerial imagery acquired in 1951 follows Hurricane Baker, a category 1 storm that made landfall on Santa Rosa Island the previous year. The beach state during 1951 is more variable than any other year, and it can be classified as LBT or RBB depending on the section of shoreline being considered. West of the Pensacola pier, the beach state is LBT, because of the slightly crescentic nearshore bar located offshore. East of the pier, the beach state is considered RBB because the nearshore bar has migrated landward with shoals from the bar almost reaching cusps along the shoreline. This alongshore transition in beach state can also be seen clearly in Fig. 2.1. Based on this transition of beach states alongshore, the area fronting Casino Beach can be assumed to have experienced lower wave energy (relative to adjacent shorelines) preceding this image than the rest of the study site for the bar to have migrated closer to the shoreline. The rip channels fronting Casino Beach have an alongshore spacing of ~200m.

Only a tropical storm strength impact was felt by Pensacola Beach in the ten years preceding the imagery of 1970 (Hurricane Camille). The TBR beach suggests that the innermost nearshore bar recently welded onto the beachface leading to a 3D bar

morphology and distinct rip channels alongshore. This accretional progression would suggest an extended period of low-energy conditions preceded this image. The welded bar cannot be digitized separately from the shoreline for the 1970 imagery and is considered a part of the shoreline feature. Rip channels along the shoreline are easily identified in the aerial imagery and are visible along the length of the study site. The rip channels tend to be oriented to the southwest, indicating a dominant wave direction from the southeast. Channels are quasi-periodic in spacing, ranging from 70 to 150m.

The 1989 imagery is an example of a RBB intermediate beach state and is characterized by a crescentic bar with an alongshore horn spacing of ~1000m. In some sections of the beach, the bar is attached to the shoreline whereas directly adjacent it is offshore by ~200m (Fig. 3.1). This image follows almost four years after a strong hurricane impact in 1985 (Hurricane Elena), followed by a tropical storm in the same year. The rip channels along the shoreline have a spacing of approximately 100 m. The 1993 imagery follows eight years after Hurricane Elena in 1985. A terrace with a small trough is visible in Fig. 3.1, as a slightly darker band of color adjacent to the shoreline. Bar 1 has a sinuous morphology with shoals meandering closer to the shoreline at approximately ~330m spacing. The shoreline is visually void of rip channels.

The beach state in 1997 is classified as LBT and follows two years after an active hurricane season in 1995 with impacts from Hurricanes Erin (Category 1) and Opal (Category 3). This high energy season may have caused the 1993 LTT beach state to be reset by the 1995 hurricane season, causing the previously welded bar to detach and migrate offshore. Bar 1 has since regained some of its sinuous morphology as it

begins to migrate landward. The bar horns have approximately ~1000m spacing. The straight shoreline has no visual rip channels.

The imagery in 2004 follows one tropical storm impact in 1997 and before the impact of Hurricane Ivan. Since the LTT beach state in 1997, bar 1 has migrated landward under low energy conditions into a TBR beach state. Bar 1 has become partially welded to the shoreline creating distinct rip channels along the length of the study site. The rip channels range in spacing between 70 and 350m. Spacing of the rip channels is widest in the east at Portofino and narrows towards Fort Pickens Gate.

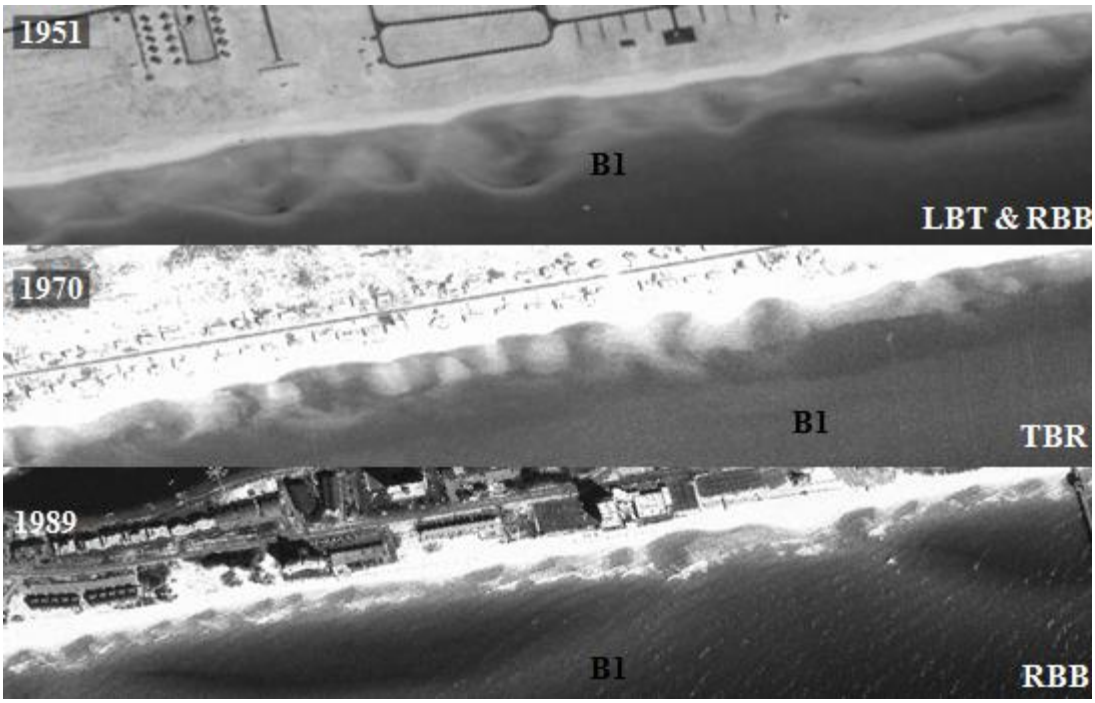

Fig. 3.1. Aerial images (at 1:6000 scale) with beach state classification according to the beach state classifications of Wright and Short (1984). B1 designates the inner bar or bar 1. B2 designates the outer bar or bar 2. Images are representative of the general beach state and not taken at the same point alongshore for each year.

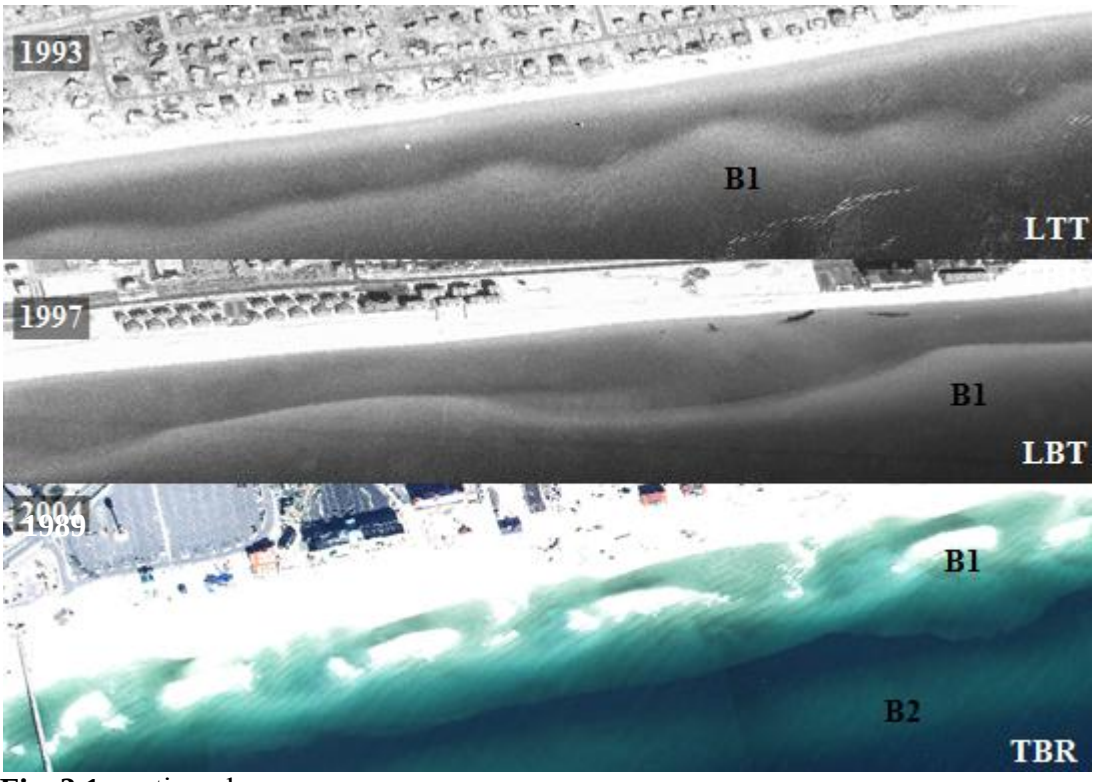

Fig. 3.1 continued.

3.2 Shoreline

A continuous wavelet transform (CWT) was created for the shoreline for each year of imagery and presented in a wavelet map (see Fig. 3.2). These continuous wavelet transforms allow for a high resolution evaluation of the signal strength to be completed continuously alongshore which facilitates the detection of multiple frequencies of variation. This quantitative approach produced frequency values that were compared directly with those of other CWT's for nearshore feature analysis.

The shoreline CWT's highlight two scales of variation for all years. A larger scale variation can be seen at period spacing of approximately 1000 m. This variation spans the length of the study site for each year and is attributed to the large scale

variation created by wave refraction over transverse ridges on the inner continental shelf (Houser et al., 2008). This ridge-scale variation has the strongest power signals within the wavelet maps for all years and is consistently present in every shoreline, regardless of beach state, storm impact or number of years since the last storm.

Superimposed on this ridge-scale variation is a higher frequency variation with a length scale of ~256 m and smaller. This variation is represented on the wavelet map as a mesh-like pattern of turquoise coloring with holes of blue, lesser power signal. This small scale variation appears to be more concentrated along discrete sections of the shoreline in every year but 1997, in which there is almost no variation at the 256m scale or smaller. Based on the average distances measured on the aerial photographs (Section 3.1), this variation is associated with rip currents. Areas of 95% confidence for both the ridge and rip scale variation can be seen along the shoreline in 1970, 1989 and 2004 within the wavelet maps as higher power signal (turquoise to yellow) surrounded by bold black lines.

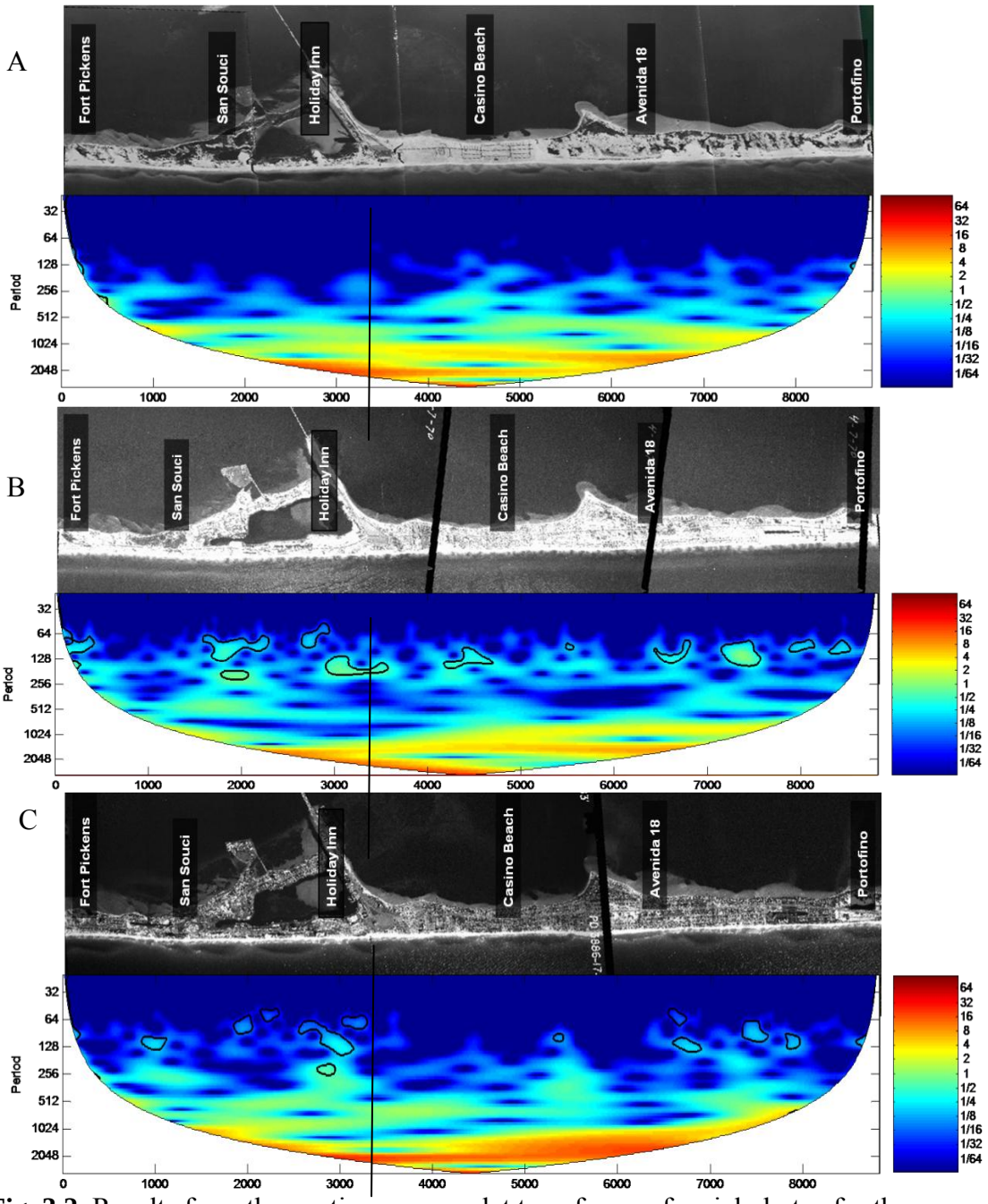

Fig. 3.2. Results from the continuous wavelet transforms of aerial photos for the shoreline. Wavelet maps are created by year a) 1951, b) 1970, c) 1989, d) 1993, e) 1997 and f) 2004. Above each wavelet map is the aerial image from which the wavelet map was created. The bold black lines indicate regions that exceed the 95% confidence interval. Areas of interest are identified in vertical text in the aerial photo. The black vertical line running from the aerial photo into the wavelet map is the Pensacola Pier and is used as a reference in the text.

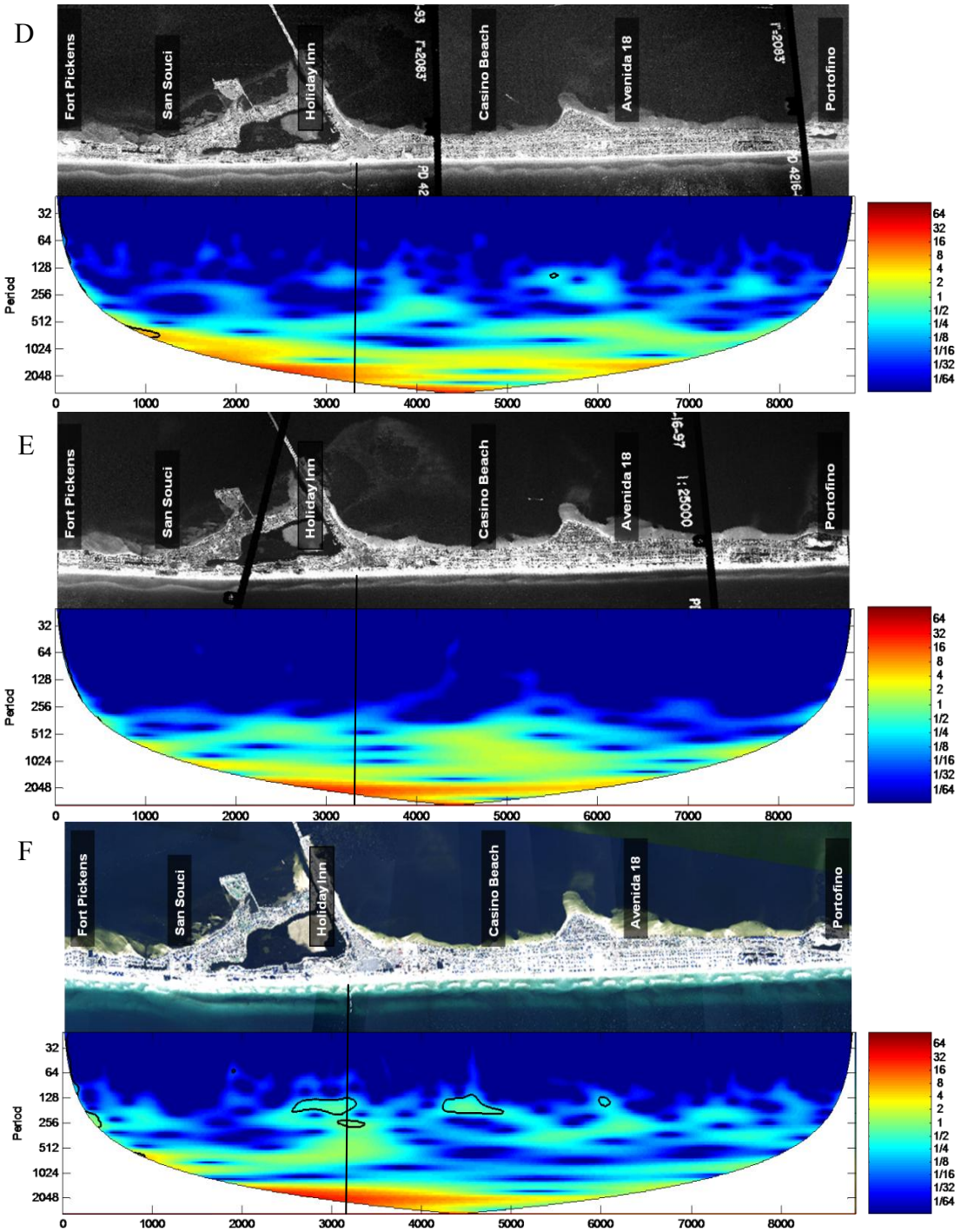

Fig. 3.2 continued.

The rip scale variation for 1951 is more distinct on the east side of the Pensacola pier, but it is not continuous along the shoreline at the ~200m spacing seen in the aerial imagery. Rather, the rip scale variation is grouped at points along the shoreline. Areas with rip-scale variation correspond with locations where bar 1 is closer to the shoreline and becomes a RBB beach state instead of LBT. With the bar closer to the shoreline, the RBB beach state is more conducive to the formation of rip channels. It appears that this quasi-periodic spacing of the rip-scale variation is forced by the ridge-scale variation seen in the higher periods of the wavelet map. In other words, there are rip clusters (statistically significant areas with strong rip-scale variation) at 1000m spacing alongshore.

The TBR morphology for 1970 shows a strong rip scale variation along the entire shoreline with areas of 95% confidence fronting Fort Pickens Gate, San Souci, the Holiday Inn, Casino Beach, Avenida 18, and Portofino, where rip-related drowning have occurred since 2000. Rip clusters are also visible in the 1989 wavelet plot at San Souci, the Holiday Inn, Casino Beach and Avenida 18. At each of these locations, bar 1 is closer to the shoreline compared to adjacent areas without rip clusters. In contrast, the low-tide terrace formation in 1993 presents a weak rip scale variation with the exception of a small but statistically significant cluster between Casino Beach and Avenida 18. No rip clusters are visible in the 1997 wavelet in which the nearshore is best characterized as LBT and 100m from the shoreline at the bar horns. The TBR beach state of 2004 exhibits a strong rip scale variation with statistically significant clusters at the Holiday Inn, Casino Beach and Avenida 18.

Global wavelets are created for each imagery year and allow the more dominant frequencies in the data series to be emphasized. Often spikes in the signal at given frequencies can help to identify the underlying mechanisms driving the data variation. The global wavelets for the shoreline (see Fig. 3.3) presents a dominant peak in frequency at 0.0003 Hz (3333m spacing), which is a frequency too small to be analyzed fully within the 8840m expanse of this study site. A longer study area would need to be analyzed in order to determine the mechanism driving this variation. Only the ridge- and rip-scale variations will be examined in this study.

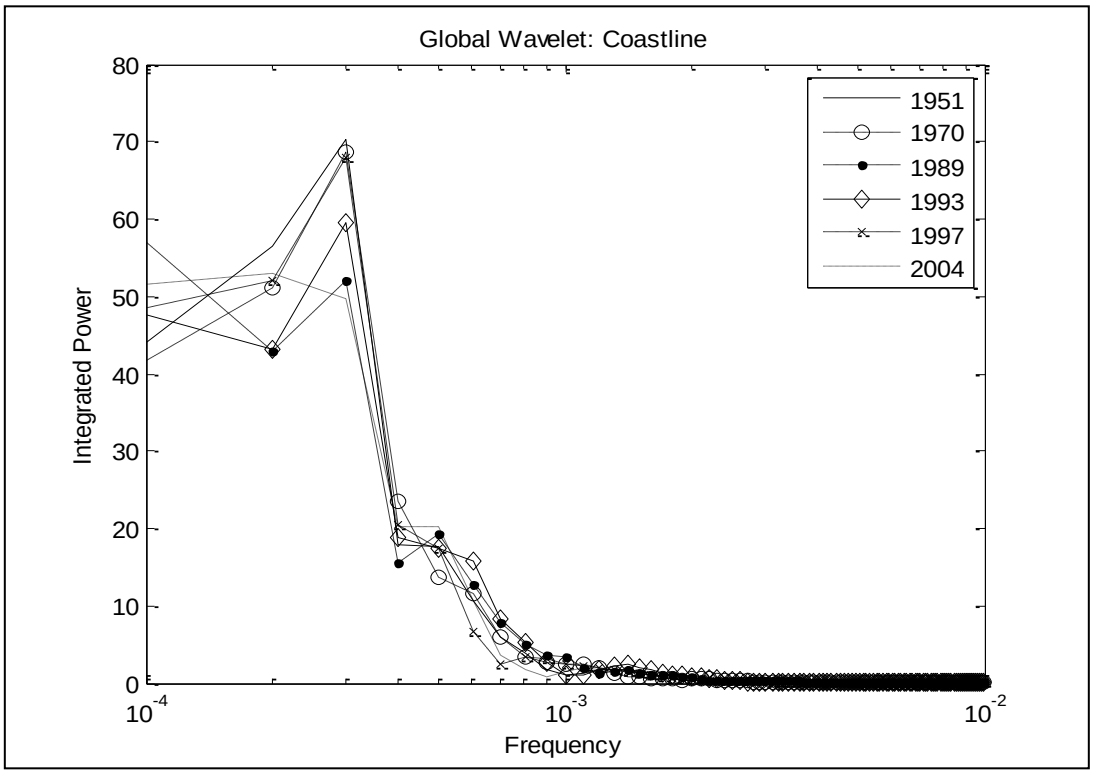

Fig. 3.3. Global wavelet of the shoreline for all years.

The remaining variation for the shoreline in the global wavelet remains relatively uniform for all years analyzed. This illustrates that the shoreline variation is relatively constant over a decadal scale. The smaller, rip scale variation cannot be extracted from the given frequencies in Fig. 3.3, but can be seen in Fig. 3.4, which highlights the integrated power for the rip-scale variation from 0.003 Hz (350m) to 0.02 Hz (50m) for the shoreline based on the rip spacing seen in the aerial imagery. Small-scale rip variations can be seen along the length of the study site for each year in Fig. 3.4. The statistically significant rip-scale clusters appear at San Souci, the Holiday Inn, Avenida 18 and points between Portofino and Avenida 18 for most years within the imagery. Again, these clusters occur at ~1000m spacing along the shoreline, which is most likely the result of wave refraction around the transverse ridges on the inner-shelf. The rip-scale variation is greatest at these rip clusters or hotspots in 1970, 1989 and 2004, which correspond with years where the beach states are either TBR or RBB and, therefore, the most conducive beach states for rip channel formation.

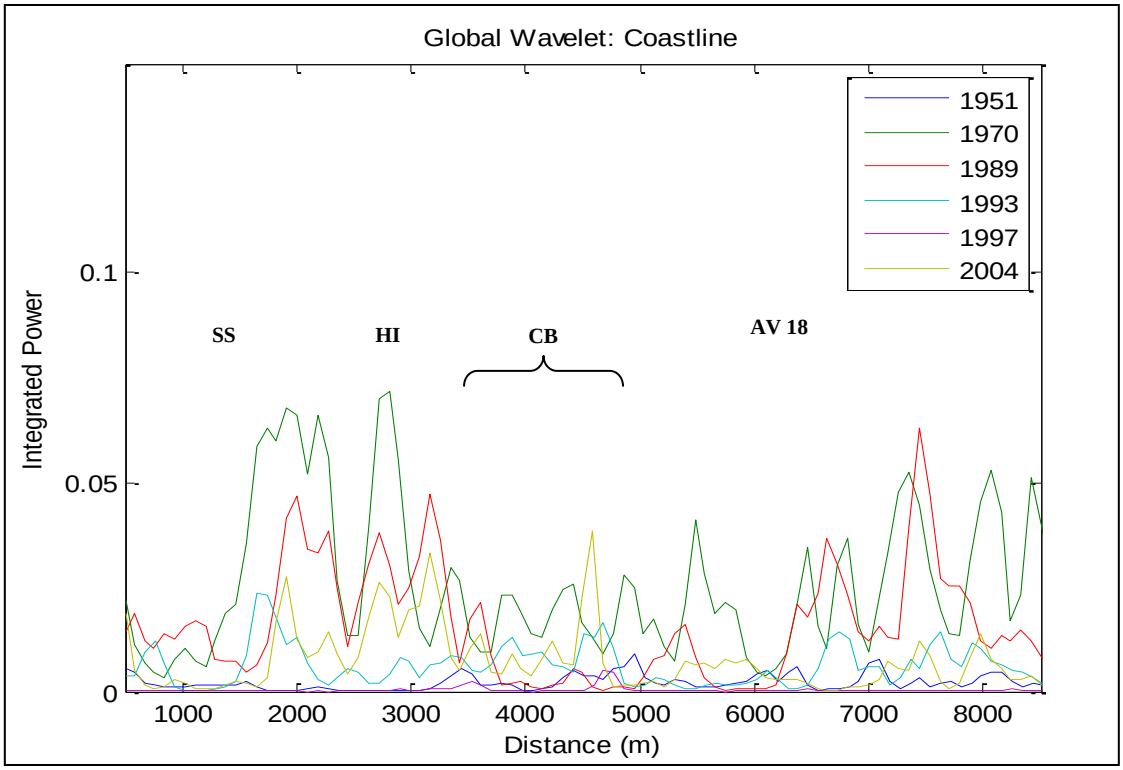

Fig. 3.4. The integrated power (of variance) for frequencies of 0.003 to 0.02 for the shoreline for all years. SS = San Souci, HI = Holiday Inn, CB = Casino Beach and AV 18 = Avenida 18.

An example of rip scale frequency can be seen in the local and global wavelet in Fig. 3.4 with areas of red color highlighting the frequency and location of the rip-scale variation at the 0.003 to 0.02 Hz range. Comparing the frequency of variation in the shoreline of 1970 to the integrated power, areas alongshore with peaks in integrated power correspond with red areas within the frequency scale. Because the frequency and integrated power scales are both able to pull out the rip-scale variation alongshore, the global and local wavelet is only used to analyze the 1970 shoreline as an example and the global wavelet will be used to analyze all remaining years.

3.3 Inner Bar

Similar to the shoreline, the dominant frequencies found in the CWT of bar 1 are also the rip (smaller) scale and ridge (larger) scale variations (Fig. 3.5). Bar 1 in 1951 has a strong, statistically significant ridge-scale variation with an alongshore spacing of ~1024m. The ridge-scale variation is coherent with a variation at its harmonic (512m) to the east of Casino Beach where the bar is closer to the shoreline. Rip-scale variations with an alongshore length scale of ~200m are superimposed on the ridge-scale variation, and exceed the 95% confidence interval over a large section of the beach. The holes in 95% confidence, shown as turquoise or blue circles within the smaller periods of the wavelet map, line up exactly with rip channels along Casino Beach where the nearshore bar is closer to the shoreline and the beach state becomes RBB (see Fig. 3.5a).

Bar 1 in 1970 shows almost no rip scale variation as it is located ~200m from the shoreline. Because, a previous nearshore bar had welded onto the beachface, the shoreline holds most of the variation as a TBR beach state. Bar 1 is starting to show a ridge scale variation at 1000m spacing and will continue to strengthen in power if in the low-energy conditions continue. The RBB beach state of 1989 presents a ridge scale variation of high power that spans the length of the study site and has the strongest power of all years for bar 1. Similar to 1951, the series of turquoise and blue circles surrounded by areas exceeding 95% confidence within the smaller periods of the wavelet map give the locations of rip channels alongshore. These rip channels are located fronting Casino Beach and Avenida 18. The low-tide terrace beach state during 1993 exhibits a strong ridge-scale variation with an area of statistical significance in the west

along Fort Pickens and San Souci and in the east along Avenida 18 and Portofino. In contrast to the previous years, the longshore bar and trough (LBT) beach of 1997 does not have a ridge-scale variation along the entire length of the study area and there is not a strong rip-scale variation. This could be attributed to Hurricane Erin and Opal's landfall two years earlier, which would have reset the beach to a LBT beach state by causing the previously welded bar to detach from the shoreline and migrate offshore creating a linear bar. Since 1995, the bar has started to migrate landward and is beginning to regain its ridge-scale variation. The rip scale variation does not return until sections of the bar migrate closer to the shoreline. In contrast, the transverse bar and rip state of 2004 produces a strong rip scale variation along the length of the study area. The blue holes in the mesh-like pattern highlights rip channel locations alongshore. The ridge-scale clustering of rip-scale variation is shown as statistically significant peaks in the lower period signal. While not all rip-scale clusters are associated with a definable rip channels, the CWT is able to identify the rip-scale variation that develops before the rip as the bar migrates landward.

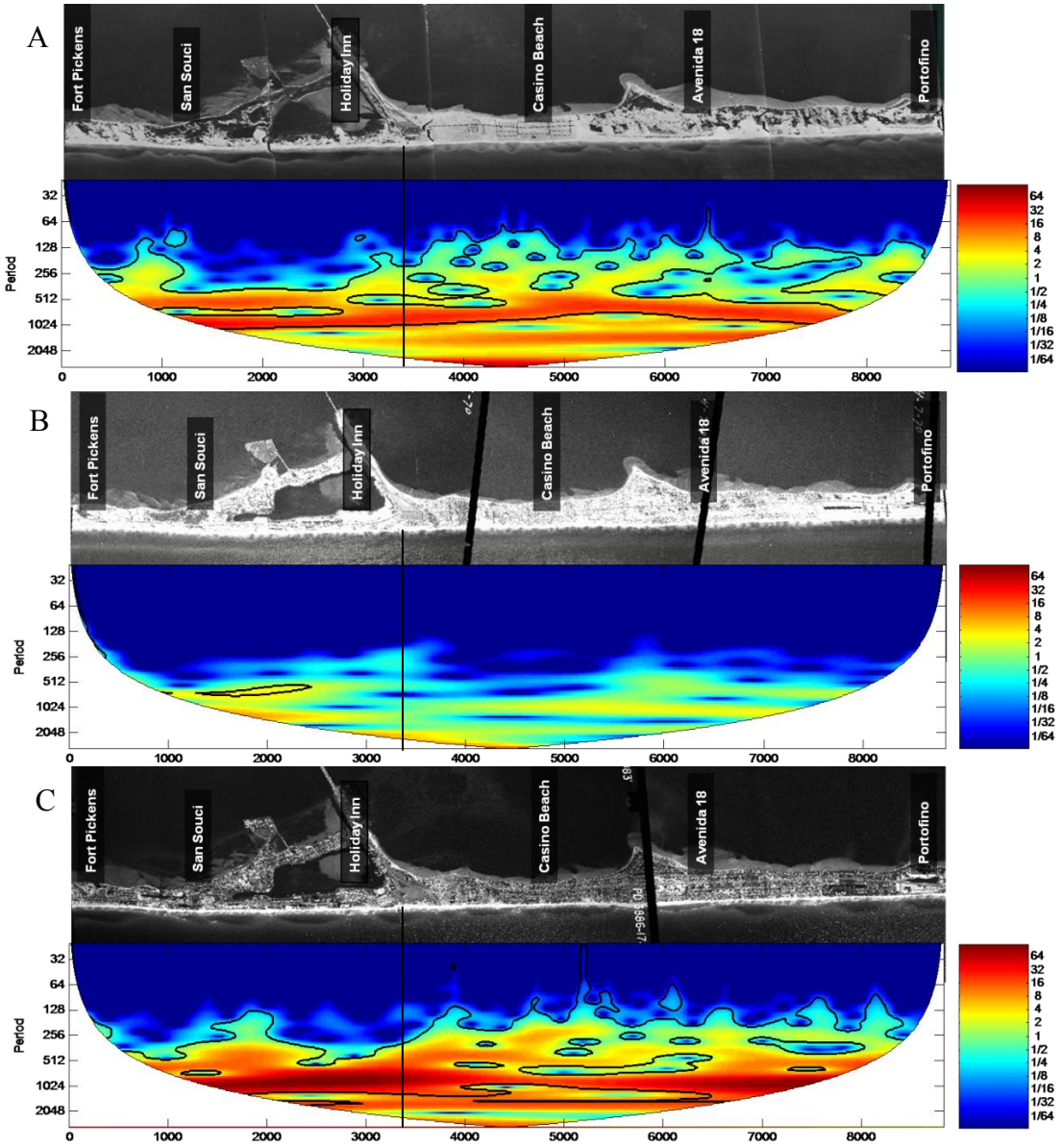

Fig. 3.5. Results from the continuous wavelet transforms of aerial photos for the inner nearshore bar. Wavelet maps are created by year a) 1951, b) 1970, c) 1989, d) 1993, e) 1997 and f) 2004. Above each wavelet map is the aerial image from which the wavelet map was created. The bold black lines indicate regions that exceed the 95% confidence interval. Areas of interest are identified in vertical text in the aerial photo. The black vertical line running from the aerial photo into the wavelet map is the Pensacola Pier and is used as a reference in the text.

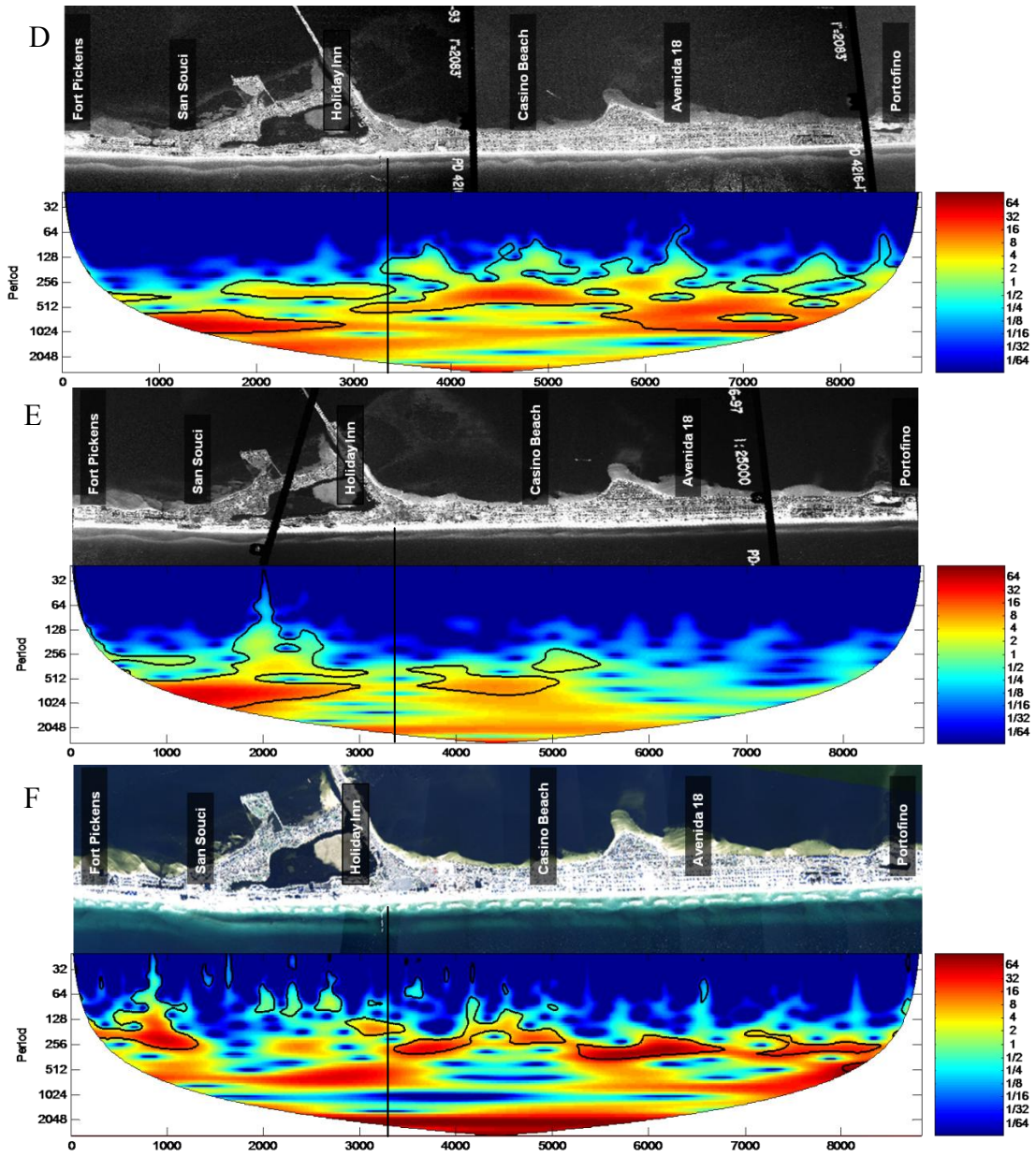

Fig. 3.5 continued.

Unlike the global wavelets for the shoreline, the global wavelets of bar 1 presents a range of frequency trends depending on the year being observed (Fig. 3.6). A jump in integrated power occurs at approximately 0.001 Hz (1,000m spacing). The signal is strongest for bar 1 during 1989 followed by 1993 and 1951. The degree of power at

0.001 Hz varies by year, which may be a factor of the respective beach states for each image. Similar to the shoreline, bar 1 exhibits a 1000m variation at which small rip-scale variations may be observed. The global wavelet in Fig. 3.6 shows that the ridge- and rip-scale variations are at approximately the same frequency in all years for bar 1. The local and global wavelet in Fig. 3.7a shows a series of peaks in the rip-scale variation (0.003 to 0.02 Hz) at points alongshore during 1989. These peaks correspond to San Souci, the majority of Casino Beach, and Avenida 18.

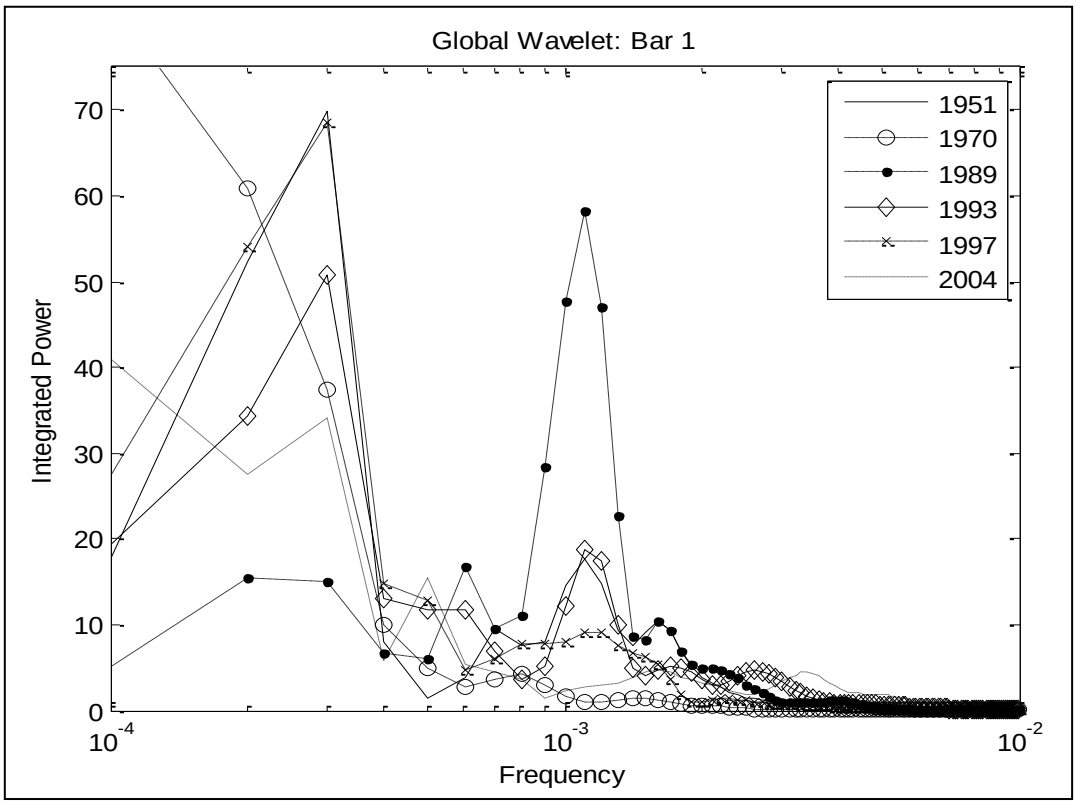

Fig. 3.6. Global wavelet for Bar 1 for all years.

The global wavelet in Fig. 3.7b shows the rip-scale variation for all years. Bar 1 for 2004 has the strongest rip-scale variation which decreases from west to east. It was noted in the aerial imagery description for 2004 that rip channel spacing increased from west to east. Therefore, there appears to be an inverse relationship between integrated power and rip channel spacing for bar 1 in 2004. Peaks within the frequency still align with San Souci, the Holiday Inn, and Avenida 18 with a series of peaks in power fronting Casino Beach. For the remaining years, clusters of rip-scale variation appear alongshore at San Souci, Casino Beach, Avenida 18 and the Holiday Inn where rip current drowning have been clustered since 2000.

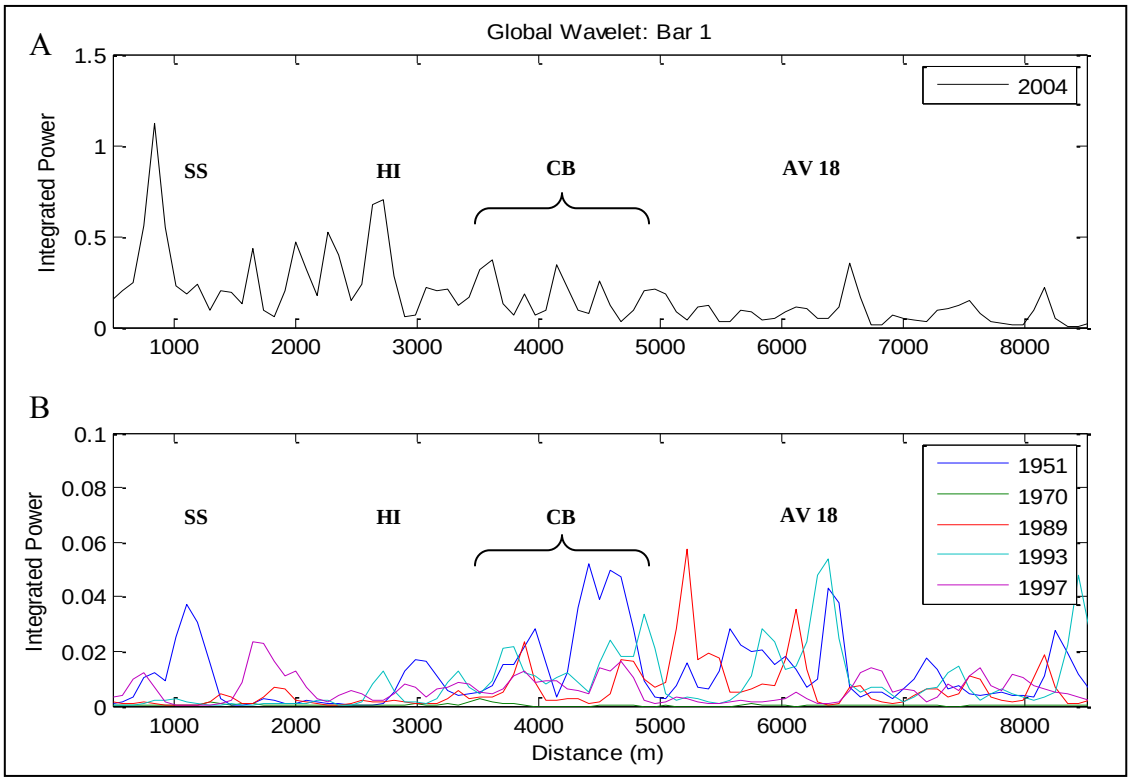

Fig. 3.7. The integrated power (of variance) for frequencies of 0.003 to 0.02 for bar 1 with 2004 (A) and all remaining years (B). SS = San Souci, HI = Holiday Inn, CB = Casino Beach and AV 18 = Avenida 18.

3.4 Outer Bar

The only year in which a second nearshore bar is present in the imagery is 2004. The 2004 CWT for bar 2 is shown in Fig. 3.8 with its aerial image. There is a visible ridge-scale variation across the entire study site at approximately 1000m spacing. This ridge spacing has high integrated power and is statistically significant across the length of the shoreline. Pockets of rip-scale variation on the east side of the pier occur at the ridge-scale spacing of ~1000m, as seen previously in bar 1 and the shoreline. The clusters of rip-scale variation are clear in the CWT as spikes of statistically significant higher power, despite bar 2 lacking any rip channels as a result of its distance from the shoreline. If low-energy conditions continued, and bar 2 migrated further landward, it can be assumed that the locations on bar 2 that line up with the 1000m ridge-scale spacing would become bar horns and be the first points to reach the shoreline. It is at these points that rip currents would form as the beach state changed to RBB at these locations. The potential future hotspots in rip current activity are located at Avenida 18, Portofino, three locations along Casino Beach (~4600m, ~5200 and ~5900m) and in line with Calle Traviesa and Avenida 23.

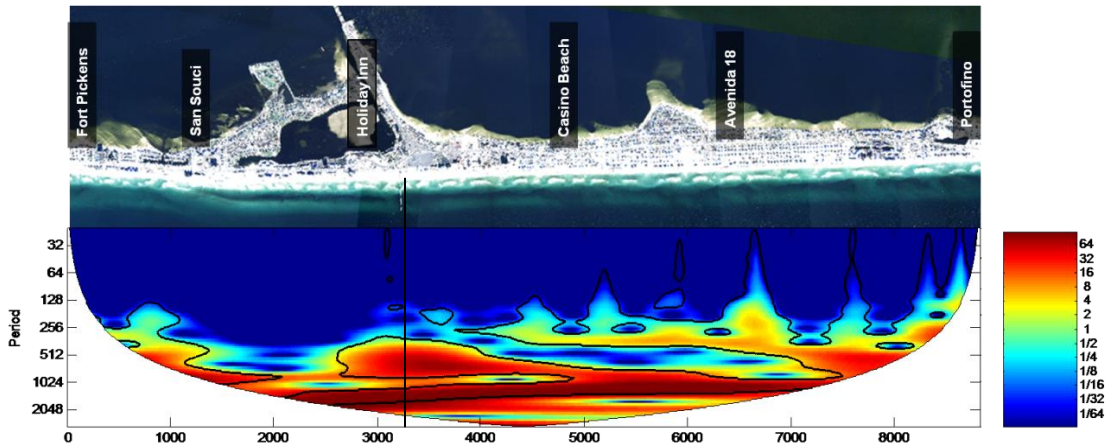

Fig. 3.8. Results from the continuous wavelet transform (bottom) for bar 2 in 2004 (top). Above each wavelet map is the aerial image from which the wavelet map was created. The bold black lines indicate regions that exceed the 95% confidence interval. Areas of interest are identified in vertical text in the aerial photo. The black vertical line running from the aerial photo into the wavelet map is the Pensacola Pier and is used as a reference in the text.

Bar 2 have dominant frequencies of 0.0005 (2000m) and 0.0008 (1250m) spacing. These frequencies are consistent with the ridge-scale spacing found along the shoreline and for bar 1 for all years of aerial imagery. Fig. 3.9 highlights the ridge-scale clustering of rip-scale variation on the east side of Pensacola Pier. This variation is not as strong as that seen for bar 1 in 2004 since the outer nearshore bar is expected to have less small scale variations within its signal.

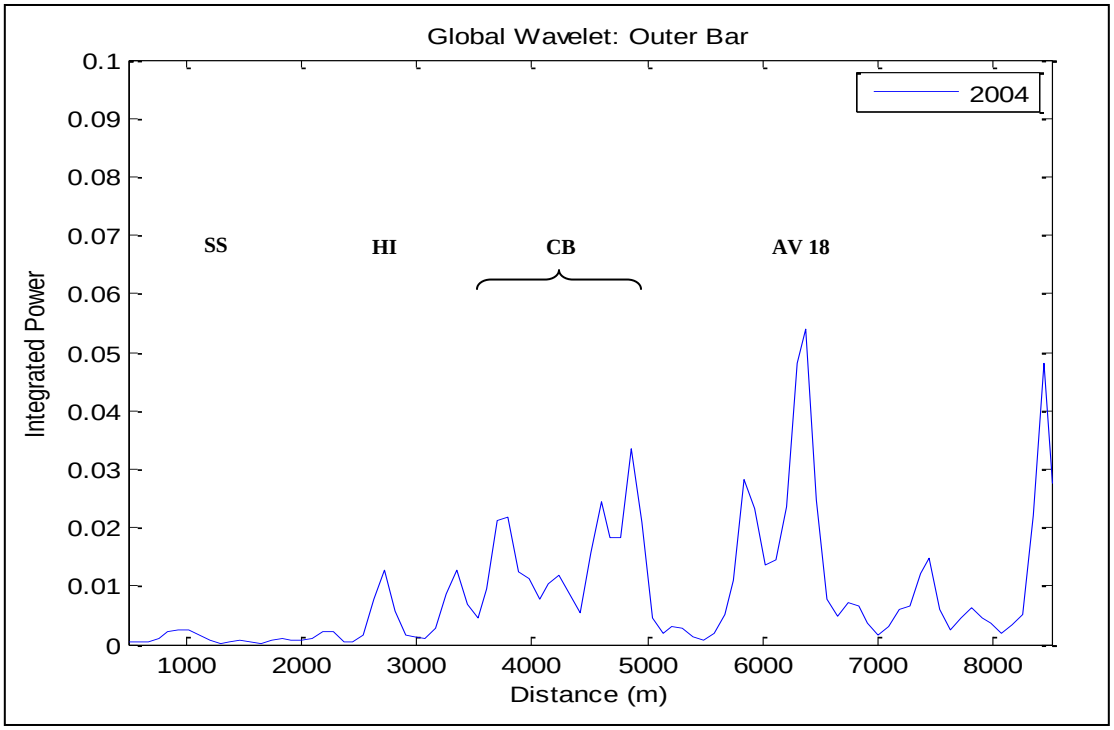

Fig. 3.9. The integrated power (of variance) for frequencies of 0.003 to 0.02 for the shoreline for all years. SS = San Souci, HI = Holiday Inn, CB = Casino Beach and AV 18 = Avenida 18.

3.5 Coherency Between Scales

Overall, two scales of frequency were seen repeating through all years of imagery, a small rip-scale variation and larger ridge-scale variation. A peak in integrated power in the global wavelet occurs for at least one of the digitized features (shoreline, bar 1 or bar 2) for each year at a frequency of ~0.001 Hz (~1,000 m). The 1,000 m variation is consistently attributed to the most seaward nearshore feature in any given year. Bar 2 in 2004 and bar 1 in 1951, 1989, 1993 and 1997 all show this 1,000m scale variation alongshore. It can be inferred that the mechanism driving this variation is the rhythmic morphology of transverse ridges on the inner continental shelf. This set of

ridges and swales have been shown to cause ~1450m scale variations in dune morphology and beach topography along the length of Santa Rosa Island (Houser et al., 2008). According to the wavelet analysis conducted from Fort Pickens Gate to Portofino in this study, the variation is ~1000m for this stretch of Santa Rosa Island.

This ridge-scale variation was observed across imagery years and nearshore features as shown in Fig. 3.10. In the shoreline, the rip-scale clusters were identified as being areas of statistical significance surrounded by a bold black line. In bar 1, the rip current locations were identified by turquoise and blue holes in the mesh-like pattern of statistical significance within the wavelet map. The detrended and digitized landward profile for the1989 inner bar is shown to emphasize how these features are driven by the same scale variation regardless of year. The horns of bar 1 in 1989, or the points closest to the shoreline, align with the rip-scale clusters in the shoreline and the rip channel locations for bar 1 in 1951. This pattern persists through every imagery year and for all digitized features. Therefore, sections of a nearshore bar that migrate landward are determined by the spacing and refraction of wave energy on the continental shelf. These 1000m spaced sections of the bar migrate landward under low-energy conditions and eventually reach the shoreline. The points at which a nearshore bar reaches the shoreline become hotspots of rip current activity as the beach state changes from LBT to RBB at these locations. These rip current hotspots typically align with Fort Pickens Gate, San Souci, the Holiday Inn, Casino Beach, Avenida 18 and Portofino.

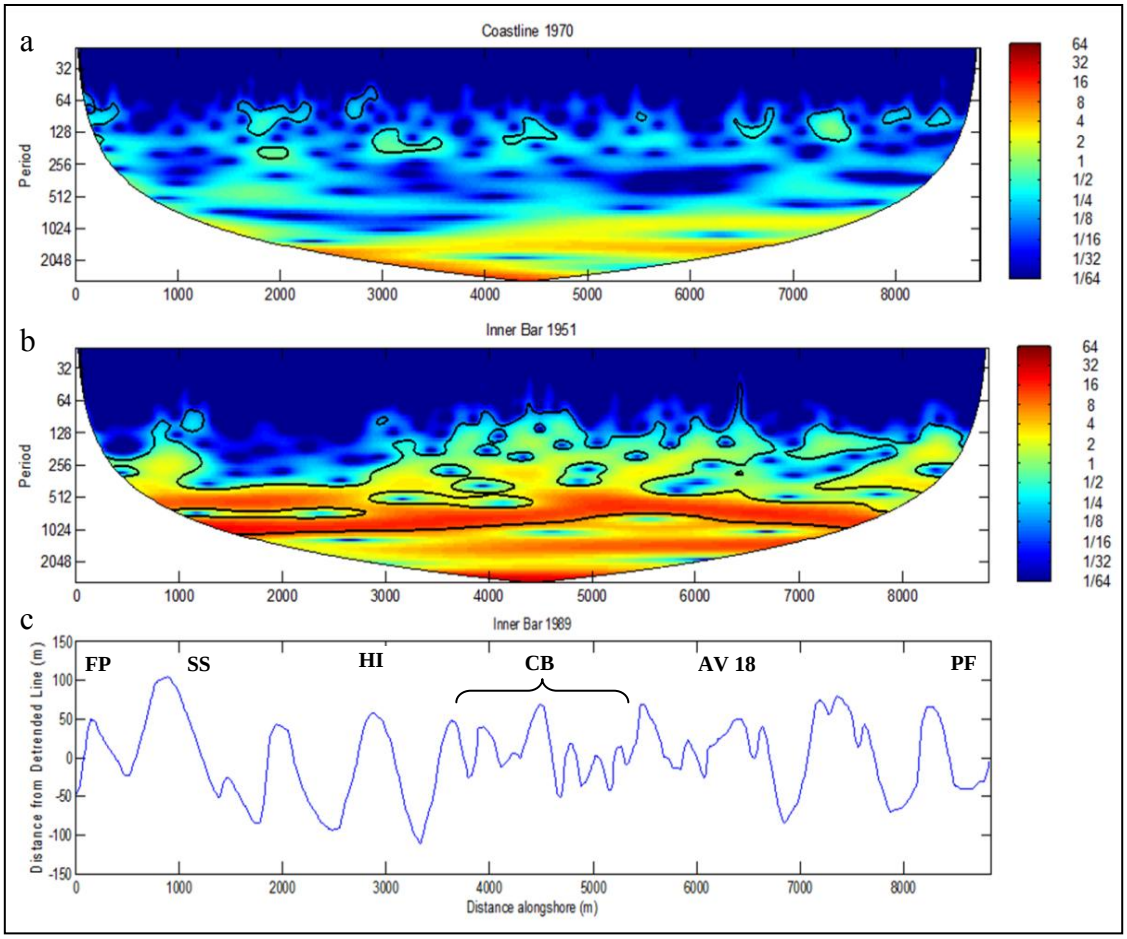

Fig. 3.10. The continuous wavelet transform of the shoreline for 1970 (a), the CWT for Bar 1 in 1951 (b) and the detrended digitized landward profile of bar 1 for 1989 (c). The bold black lines indicate regions that exceed the 95% confidence interval. SS = San Souci, HI = Holiday Inn, CB = Casino Beach and AV 18 = Avenida 18.

CHAPTER IV

DISCUSSION

Wavelet analysis and specifically continuous wavelet transforms (CWTs) is a powerful analysis technique to identify the dominant periods of variation within a nearshore feature that are rarely stationary alongshore. Frequencies can be compared directly with those of other CWT's to compare and contrast between imagery years, beach states, and storm impacts. In this study, CWTs are used to identify locations and times where rip current systems develop along the shoreline of Pensacola Beach, Florida. While generally considered a low-energy coastline compared to the west coast and Eastern Seaboard, Pensacola Beach has been identified as one of the most hazardous beaches in the United States (The Tuscaloosa News, 2002) and there have been six rip-current related drowning since 2003. The ability to identify hazardous times (within the bar cycle) and locations alongshore is a significant improvement on the National Weather Service rip forecast that is based solely on meteorological forcing and assumes that the rip hazard is uniform alongshore. Results of the present study suggest that the rip hazard at Pensacola Beach is controlled by the transverse ridges on the inner-shelf and dependent on bar migration within the bar cycle.

The beach-state and the rip hazard could be qualitatively described visually from the aerial and satellite photographs and using the Wright and Short (1984) classification, but the scale of that variation (if visually discernible) is difficult to assess. The wavelet maps produced from the continuous wavelet transforms not only supported the beach

state classifications given to the aerial photographs for each year but provide important detail about the scale and location of that variation. In general, variability in the bar and shoreline morphology was identified at alongshore length scales of < 256 m and between 1000 and 2000 m, which are described as being rip- and ridge-scale variations respectively. The relative importance of the rip- and ridge-scale variation depended on the point in the bar cycle that the photograph was taken. For example, the longshore bar and trough morphology of 1997 (see Fig. 3.5e) has a more subdued rip-scale morphology and was largely dominated by ridge-scale variation because of its linear shoreline and nearshore bar located 100m offshore having a slightly sinuous alongshore morphology. In contrast, the transverse bar and rip morphology of 2004 (see Fig. 3.5f) produced a dominant, rip-scale morphology with clustered pockets of statistical significance along the shoreline at ridge-scale spacing. The 1997 imagery follows two years after Hurricane Opal (Category 3 hurricane). The 2004 imagery follows seven years after Hurricane Opal with only an additional tropical storm affecting the area.

A further example of the ridge- and rip-scale variations is presented in Fig. 3.5a for 1951. The larger ridge-scale variation has an alongshore length scale of ~1000m spacing in addition to a smaller rip-scale variation that is clustered along the shoreline in a RBB beach. Similar results were collected by Ruessink et al. (2006) where higher power signal was found at two wavelengths within the wavelet maps along portions of the shoreline for an inner and outer bar. Their wavelet maps also showed larger scale undulating inner bar variability with superimposed small-scale rip current variation with an alongshore length scale between 100-200m. This length scale is consistent with the

rip-scale variation of < 256 m in the present study. In this respect, the present study supports Ruessink et al. (2006) and suggests that bar morphology exhibits different scales of variation.

In general, the shoreline and bar morphology is dominated by the relatively low-frequency ridge-scale variation (Fig. 3.6). This variation, seen in all years of aerial imagery, is attributed to transverse ridges on the inner continental shelf (Houser et al., 2008). The focusing and defocusing of wave energy around a geologic framework and the bathymetry of offshore regions have been shown in several studies to determine a coastal response (Demarest and Leatherman, 1985; Riggs et al., 1995; Browder and McNinch, 2006). The ridges are also an important control on alongshore recovery, vegetation, island width, overwash penetration and dune height before a storm (Houser and Hamilton, 2009). While Houser et al. (2008) found a ~1450m variation in the shoreline erosion, dune morphology and overwash penetration attributed to the transverse ridge forcing, the study site used was a 11 km stretch of Santa Rosa Island and was estimated using traditional fourier analysis. In this respect, this length scale is not representative of the transverse ridge morphology in the 8.8 km length of the shoreline examined in this study. It appears that the transverse ridges fronting Pensacola Beach have a smaller spacing and are responsible for a higher frequency variation in the nearshore morphology and the shoreline. The integrated power for the ridge-scale variation along the shoreline and bar 1 is not consistent from year to year. However, there appear to be no clear relationships of the ridge-scale variation and the tropical storms and hurricanes that made landfall in the area. This suggests that other variables,

such as frontal storms or distance storm tracks are controlling the bar cycle and the integrated power of the ridge-scale variation. This raises an interesting question of what is causing the ridge-scale variation to be stronger during different years, that is not driven by the beach state or storm impact during those years?

While no clear relationship was identified between the extreme storms, the bar cycle and the amount of ridge- and rip-scale variation, the rip-scale variation is nonetheless tied to the bar cycle. Rip currents were most numerous during transverse bar and rip beach states which were present in 1970 and 2004. Drownings from 2003 along Pensacola Beach collected by the U.S. Lifesaving Association and analyzed in Houser et al. (2010), show five drownings for the year. Two drownings were roughly located within my study area at ~1150m (San Souci), one drowning at ~2300m (Holiday Inn) and two additional drownings at ~4000m (Casino Beach). These three drowning locations align with three statistically significant, high power rip clusters at these locations for the bar 1 CWT in 2004 (see Fig. 3.5). The alongshore correspondence between the rip-scale clusters and the rip-related drowning demonstrates the ability of CWT's to accurately identify hotspots of rip current activity. Unfortunately, drowning statistics with exact location data have only been collected since 2003 for Santa Rosa Island and, therefore, it is difficult to compare to the other beach states and aerial imagery used in the present study. An archival search of drowning data is recommended to identify the historical pattern of drowning relative to the changes in beach state through the bar cycle.

The rip-scale clusters highlighted by the CWT's have an alongshore spacing of ~1000 m, similar to the ridge-scale variation. In general, the rip clusters were found within ~250m or less of the rip current hotspot locations previously identified and where the nearshore bars were closest if not attached to the shoreline. While the location of the rip clusters appears to be coherent with the ridge-scale variation, the exact locations of the clustered rip-scale variation did not line up exactly between different years alongshore. This suggests the transverse ridge spacing forces the alongshore location of rip cluster spacing or hotspot locations, but the control on the exact location varies from year to year. These results support previous studies which found rip current spacing was highly variable alongshore (Holman et al., 2006). What drives the exact locations of rip current hotspots is currently unknown but is possibly a result of wave conditions, longshore current or other factors. For example, during a field experiment in August 2011 San Souci was chosen as the location of a rip current study. Upon arrival, it was found that rip channels were not present in front of San Souci but 100-200 m down the coastline.

A rip current hazard depends on the morphology of the coastline as well as people being present on the beach. If there are no people on Pensacola Beach, then the rip currents are no longer a hazard. Considering Pensacola Beach receives over 200,000 vehicle visits even in the less popular winter months, the majority of the rip hazard is defined by the number of rip channels along the coastline. While the greatest number of rip currents were found in a transverse bar and rip beach morphology, the most dangerous conditions may potentially occur during a rhythmic bar and beach

morphology as defined by Wright and Short (1984) (Fig. 1.5). Rip current hotspots were located at the horns of nearshore bars at points where they reach the shoals along the shoreline in years with RBB morphologies. This may potentially be dangerous because prior to the horns of the nearshore bars reaching the shoreline, there is a relatively weak rip-scale variation associated with the LBT morphology (see Fig. 3.5e). Assuming an accretionary sequence continues, RBB morphologies typically had a stronger rip-scale strength variation than those of a LBT. Potentially, during the course of a few months, a period of few rip currents may quickly change to a period of clustered hotspots of strong rip current activity alongshore. This can be seen when comparing the CWT of the inner bar for the LBT morphology in 1997 (Fig. 3.5e) to the CWT of the inner bar for the TBR morphology in 2004 (Fig. 3.5f). The LBT morphology has very little rip-scale variation while the RBB morphology is dominated by the rip-scale variation at ridge-scale spacing along the shoreline. However, recent studies have shown that inner bars exhibit the least amount of time in the RBB beach state over the other beach states and in a recent study, the RBB beach state was only seen for the inner bar during 1 day of the 8 week study (Ruessink et al., 2006).

The clustering of the rip current hotspots and the ability of wavelet analysis to identify those areas is important for coastal managers and lifeguards located at Pensacola Beach. For example, using wavelet analysis, lifeguards could move their lifeguard stands into areas of rip current hotspots in an effort to monitor these higher risk areas more closely to prevent future drowning. These alongshore hot spots can be seen in the shoreline in 1989 (Fig. 3.2c), where clustered areas of statistical significance are

distributed through the smaller periods of the wavelet map at ~1000m spacing. The RBB morphology has a smaller number of rip channels present, but may present a greater hazard because of their discrete locations. The majority of the shoreline is free of rip channels except for the ~100m stretches of shoreline where the bar has migrated landward and created a morphology conduce to the development of rip currents. These discrete points along the shoreline coincide with beach access points along Pensacola Beach that coincide with the troughs in transverse ridges (Houser et al., 2011). This becomes an issue for coastal management as recent studies have found that beach-users typically occupy a space 100 to 250m from beach access points (Jimenez et al., 2007), essentially attracting them to the locations with the greatest rip current hazard.

A reasonable estimate of where the rip current hotspots will develop could potentially be derived from the CWT's of the outermost bar before the bars weld to the shoreline. Despite the fact that bar 2 was located 200m from the shoreline and was void of rip currents, the ~1000m spacing in the rip-scale variation was seen within the wavelet map. These clustered rip current hotspots lined up with the previously defined hotspots of rip current activity at Fort Pickens Gate, San Souci, Holiday Inn, Casino Beach, Avenida 18 and Portofino. While the 1000m variation is predetermined by the spacing of the continental shelf's transverse ridges, CWT's may provide a smaller distance range alongshore at which future rip current activity may occur. This theory cannot be tested further in this study as Pensacola Beach was heavily impacted by Hurricane Ivan (Category 3) and reset this shoreline only six months later. While the rip hotspots will most likely develop landward of the swales where wave heights are

relatively small, the exact position of the rip hotspots depends on the incident forcing driving the bars landward.

CHAPTER V

CONCLUSIONS

Wavelet analysis is a valuable tool in the analysis of non-stationary, nearshore features, because it allows a spatial signal to be decomposed and localized in both frequency (scale) and time domains simultaneously. Multiple frequencies of variation could be identified within the spatial series and compared directly between years and nearshore features. Two frequencies of variation dominated all nearshore features at Pensacola Beach, Florida. A larger, ridge-scale variation at ~1000m spacing was observed in the continuous wavelet transforms in all years of imagery. This variation is caused by wave focusing (troughs) and defocusing (ridges) along transverse ridges on the inner continental shelf. Superimposed on this variation is a smaller rip-scale variation that is clustered along the shoreline. The spacing of these clusters is ~1000 m and suggests that the rip current hotspots are geologically forced by the ridge and swale features on the inner-shelf.

Rip currents were most numerous and extended along the length of the study site during transverse bar and rip beach states (1970 and 2004) but were clustered at 1000m intervals under a rhythmic bar beach morphology forced by the ridge-scale variation. There is not a clear relationship between storm impacts and rip current activity as a greater number and higher density of images would need to be analyzed to capture the migration behavior of the nearshore bars between storms.

Clusters in rip-scale variation or hotspots in rip current activity were located using continuous wavelet transforms in the following locations between years: Fort Pickens Gate, San Souci, Holiday Inn, Casino Beach, Avenida 18 and Portofino. This clustering of rip-scale variation is repeated through all years of aerial imagery at these locations regardless of beach state. While the ridge-scale variation forces clusters of rip current activity into these locations alongshore, the continuous wavelet transforms of the outer or secondary bars could possibly provide more specific locations (< 250m) at which rip current clustering will occur in the future as the bar continues to migrate landward under low-energy conditions.

REFERENCES

Aagaard, T., Davidson-Arnott, R., Greenwood, B., Nielsen, J., 2004. Sediment supply from shoreface to dunes: linking sediment transport measurements and long-term morphological evolution. Geomorphology 60, 205-224.

Aagaard, T., Greenwood, B., Nielsen, J., 1997. Mean currents and sediment transport in a rip channel. Marine Geology 140, 25-45.

Aagaard, T., Kroon, A., Greenwood, B., Hughes, M.G., 2010. Observations of offshore bar decay: sediment budgets and the role of lower shoreface processes. Continental Shelf Research 30, 1497-1510.

Aagaard, T., Nielsen, J., Greenwood, B., 1998. Suspended sediment transport and nearshore bar formation on a shallow intermediate-state beach. Marine Geology 148, 203-225.

Aarninkhof, S.G.J., Hinton, C., Wijnberg, K.M., 1998. On the predictability of nearshore bar behaviour. In: Proceedings of 26th International Conference on Coastal Engineering. ASCE: New York, pp. 2409-2422.

Bazartseren, B., Holz, K.P., 2002. Coastal morphological data reduction using a wavelet and principal component analysis. In: Proceedings of the 5th International Conference of Hydro-Science and Engineering. ICHE: Warsaw, Poland, pp. 145-155.

Birkemeier, W.A., Holland, K.T., 2001. The Corps of Engineers' Field Research Facility: More than two decades of coastal research. Shore and Beach 69, 3-12.

Bowen, A.J., 1969. Rip currents 1: Theoretical investigations. Journal of Geophysical Research 74, 5467-5478.

Bowen, A.J., Inman, D.L., 1969. Rip currents 2: Laboratory and field observations. Journal of Geophysical Research 74, 5479-5490.

Brander, R.W., Short, A.D., 2001. Flow kinematics of low-energy rip current systems. Journal of Coastal Research 17, 468-481.

Brander, R.W., Short, A.D., 2000. Morphodynamics of a large-scale rip current system at Muriwai Beach, New Zealand. Marine Geology 165, 27-39.

Brander, R.W., 1999. Field observations on the morphodynamic evolution of a low-energy rip current system. Marine Geology 157, 199-217.

Browder, A.G., McNinch, J.E., 2006. Linking framework geology and nearshore morphology: Correlation of paleo-channels with shore-oblique sandbars and gravel outcrops. Marine Geology 231, 141-162.

Calvete, D., Coco, G., Falques, A., Dodd, N., 2007. (Un)predictability in rip channel systems. Geophysical Research Letters 34, pp. 1-5.

Castelle, B., Bonneton, P., Dupuis, H., Senechal, N., 2007. Double bar beach dynamics on the high-energy meso-macrotidal French Aquitanian Coast: A review. Marine Geology 245, 141-159.

Castelle, B., Ruessink, B.G., Bonneton, P., Marieu, V., Bruneau, N., Price, T.D., 2010. Coupling mechanisms in double sandbar systems. Part 2: Impact on alongshore variability of inner-bar rip channels. Earth Surface Processes and Landforms 35, 771-781.

Coco, G., Bryan, K.R., Green, M.O., Ruessink, B.G., Turner, I.L., van Enckevort, I.M.J., 2005. Video observations of shoreline and sandbar coupled dynamics. Proceedings of Coast and Ports 2005. Adelaide, pp. 471-476.

Coco, G., Huntley, D.A., O'Hare, T.J., 2001. Investigation of a self-organisation model for beach cusp formation and development. Journal of Geophysical Research 105 21991-22002.

Coco, G., Murray, A.B., 2007. Patterns in the sand: From forcing templates to self-organization. Geomorphology 91, 271-290.

Damgaard, J., Dodd, N., Chesher, T., 2002. Morphodynamic modeling of rip channel growth. Coastal Engineering 43, 199-221.

Deigaard, R., Drønen, N., Fredsøe, J., Jensen, J.H., Jørgensen, M.P., 1999. A morphological stability analysis for a long straight barred coast. Coastal Engineering 36, 171-195.

Demarest, J.M., Leatherman, S.P., 1985. Mainland influence on coastal transgression – Delmarva Peninsula. Marine Geology 63, 19-33.

Elsayed, M., 2010. An overview of wavelet analysis and its application to ocean wind waves. Journal of Coastal Research 26, 535-540.

Farge, M., 1992. Wavelet transforms and their applications to turbulence. Annual Review of Fluid Mechanics 24, 395-457.

Fletemeyer, J., Leatherman, S., 2010. Rip currents and beach safety education. Journal of Coastal Research 26, 1-3.

Gallagher, E.L., Elgar, S., Thornton, E.B., 1998. Observations and predictions of megaripple migration in a natural surf zone. Nature 394, 165-168.

Gensini, V., Ashley, W., 2010. An examination of rip current fatalities in the United States. Natural Hazards 54, 159-175.

Greenwood, B., Davidson-Arnott, R.G.D., 1979. Sedimentation and equilibrium in wave-formed bars: A review and case study. Canadian Journal of Earth Sciences 16, 312-332.

Grossman, A., Morlet, J., 1985. Decomposition of functions into wavelets of constant shape and related transforms. In: L. Streit (Editor), Mathematics + Physics, Lectures on Recent Results. World Scientific: Singapore, 135-165.

Guza, R.T., Inman, D.L., 1975. Edge waves and beach cusps. Journal of Geophysical Research 80, 2997-3012.

Haas, K.A., Svendsen, I.A., Brander, R.W., Nielsen, P., 2003. Modeling of a rip current system on Moreton Island, Australia. In: Proceedings 28th International Conference on Coastal Engineering 2002. American Society of Civil Engineers: New York, pp. 784-796.

Hino, M., 1974. Theory on formation of rip-current and cuspidal coast. Coastal Engineering Japan 17, 23-37.

Holman, R.A., Symonds, G., Thornton, E.B., Ranasinghe, R., 2006. Rip spacing and persistence on an embayed beach. Journal of Geophysical Research 111, pp. *-*. DOI: 10.1029/2005/JC002965.

Houser, C., Barrett, G., Labude, D., 2011. Alongshore variation in the rip current hazard at Pensacola Beach, Florida. Natural Hazards 57, 501-523.

Houser, C., Greenwood, B., 2005. Profile response of a lacustrine multiple barred nearshore to a sequence of storm events. Geomorphology 69, 118-137.

Houser, C., Hapke, C., Hamilton, S., 2008. Controls on the coastal dune morphology, shoreline erosion and barrier island response to extreme storms. Geomorphology, 100, 223-240.

Houser, C., Hamilton S., 2009. Sensitivity of post-hurricane beach and dune recovery to event frequency. Earth Surface Processes & Landforms 34, 613-628.

Houser, C., Mathew, S., 2011. Alongshore variation in foredune height in response to transport potential and sediment supply: South Padre Island, Texas. Geomorphology 125, 62-72.

Hsu, T.J., Elgar, S., Guza, R.T., 2006. Wave-induced sediment transport and onshore sandbar migration. Coastal Engineering 53, 817-824.

Huntley, D.A., Hendry, M.D., Haines, J., Greenidge, B., 1988. Waves and rip currents on a Caribbean pocket beach, Jamaica. Journal of Coastal Research 4, 69-79.

Huntley, D.A., Short, A.D., 1992. On the spacing between observed rip currents. Coastal Engineering 17, 211-225.

Hyne, N.J., Goodell, H.G., 1967. Origin of the sediments and submarine geomorphology of the inner continental shelf off Choctawhatchee Bay, Florida. Marine Geology 5, 299-313.

James, R.J., 2000. From beaches to beach environments: Linking the ecology, human-use and management of beaches in Australia. Ocean and Coastal Management 43, 495-514.

Jimenez, J.A., Osorio, A., Marino-Tapia, I., Davidson, M., Medina, R., Kroon, A., Archetti, R., Ciavola, P., Aarnikhof, S.G.J., 2007. Beach recreation planning using video-derived coastal state indicators. Coastal Engineering 54, 507-521.

Jordan, D.A., Hajj, M.R., Tieleman, H.W., 1997. Characterization of turbulence scales in the atmospheric surface layer with the continuous wavelet transform. Journal of Wind Engineering and Industrial Aerodynamics 69, 709-716.

Komar, P.D., 1976. Phenocryst interactions and velocity profile of magma flowing through dikes or sills. Geological Society of America Bulletin 87, 1336-1342.

Lafon, V., Dupuis, H., Butel, R., Castelle, B., Michel, D., Howa, H., De Melo Apoluceno, D., 2005. Morphodynamics of nearshore rhythmic sandbars in a mixed-energy environment (SW France): II. Physical forcing analysis. Estuarine, Coastal and Shelf Science 65, 449-462.

Lascody, L.L., 1998. East central Florida rip current program. National Weather Digest 22, 25-30.

Li, Y., Lark, M., Reeve, D., 2005. Multi-scale variability of beach profiles at Duck: A wavelet analysis. Coastal Engineering 52, 1133-1153.

Liu, P.C., 1994. Wavelet spectrum analysis and ocean wind waves. Wavelets in Geophysics. In: E. Foufoula-Georgious and P. Kumar, Eds., Academic Press, San Diego, CA, 151-166.

Longuet-Higgins, M.S., Stewart, R.W., 1964. Radiation stress in water waves, a physical discussion with applications. Deep-Sea Research 11, 529-563.

Lushine, J.B., 1991a. A study of rip current drowning and weather related factors. National Weather Digest 16, 13-19.

Lushine, J.B., 1991b. Rip currents: Human impact and forecastability. In: Proceedings Coastal Zone ASCE, New York, 3558-3569.

MacMahan, J., Thornton, E.B., Stanton, T.P., Reniers, A.J.H.M., 2005. RIPEX – rip currents on a shore-connected shoal beach. Marine Geology 218, 113-134.

MacMahan, J., Reniers, A.J.H.M., Thornton, E.B., Stanton, T., 2004. Infragravity rip current pulsations. Journal of Geophysical Research 109, pp. *-*.

McKenzie, P., 1958. Rip current systems. Journal of Geology 66, 103-113.

Masselink, G., 2004. Formation and evolution of multiple intertidal bars on macrotidal beaches: Application of a morphosdynamic model. Coastal Engineering 51, 713-730.

Plant, N.G., Freilich, M.H., Holman, R.A., 2001. Role of morphologic feedback in surf zone sandbar response. Journal of Geophysical Research 106, 973-989.

Reniers, E., Roelvink, D., Thornton, E.B., 2004. Morphodynamic modeling of an embayed beach under wave group forcing. Journal of Geophysical Research 109, pp. *-*. DOI:10.1029/2002JC001586.

Riggs, S.R., Cleary, J.C., Snyder, S.W., 1995. Influence of inherited geologic framework on barrier shoreface morphology and dynamics. Marine Geology 126, 231-234.

Ruessink, B.G., Coco, G., Ranasinghe, R., Turner, I.L., 2006. A cross-wavelet study of alongshore nonuniform nearshore sandbar behavior. In: Proceedings of the IEEE International Joint Conference on Neural Networks, Vancouver, Canada, 4310-4317.

Ruessink, B.G., Houwman, K.T., Hoekstra, P., 1998. The systematic contribution of transporting mechanisms to the cross-shore sediment transport in water depths of 3 to 9 m. Marine Geology 152, 295-324.

Ruessink, B.G., Kroon, A., 1994. The behaviour of a multiple bar system in the nearshore zone of Terschelling, the Netherlands: 1965-1993. Marine Geology 121, 187-197.

Ruessink, B.G., Miles, J.R., Feddersen, F., Guza, R.T., Elgar, S., 2001. Modeling the alongshore current on barred beaches. Journal of Geophysical Research 106, 22451-22463.

Ruessink, B.G., Terwindt, J.H.J., 2000. The behaviour of nearshore bars on the time scale of years: A conceptual model. Marine Geology 163, 289-302.

Ruessink, B.G., Coco, G., Ranasinghe, R., Turner, I.L., 2007. Coupled and noncoupled behavior of three-dimensional morphological patterns in double sandbar systems. Journal of Geophysical Research 112, pp. 1-11, DOI: 10.1029/2006JC003799.

Ruessink, B.G., van Enckevort, I.M.J., Kingston, K.S., Davidson, M.A., 2000. Analysis of observed two- and three- dimensional nearshore bar behavior. Marine Geology 169, 161-183.

Shepard, F.P., 1950. Longshore current observations in southern California: Technical Memorandum No. 13, Beach Erosion Board, Corps of Engineers, Washington D.C., 31 p.

Shepard, F.P., 1952. Revised nomenclature for depositional coastal features. Bulletin of the American Association of Petroleum Geology 36, 1902-1912.

Shepard, F.P., Inman, D.L., 1950. Nearshore water circulation related to bottom topography and wave refraction, Trans-American Geophysical Union, AGU, 31, 196-212.

Short, A.D., 1985. Rip-current type, spacing and persistence, Narrabeen Beach, Australia. Marine Geology 65, 47-71.

Short, A.D., Brander, R.W., 1999. Regional variations in rip density. Journal of Coastal Research 15, 813-822.

Short, A.D., Hogan, C.L., 1994. Rip current and beach hazards: Their impact on public safety and implications for coastal management. Journal of Coastal Research, SI 12, 197-209.

Short, A.D., Trembanis, A.C., 2004. Decadal scale patterns in beach oscillation and rotation Narrabeen Beach, Australia; – Time series, PCA and wavelet analysis. Journal of Coastal Research 20, 523-532.

Sonu, C.J., 1972. Field observation of nearshore circulation and meandering currents. Journal of Geophysical Research 77, 3232-3247.

Sonu, C.J., 1973. Three-dimensional beach changes. Journal of Geology 81, 42-64.

Stive, M.J.F., Wind, H.G., 1986. Cross-shore mean flow in the surf zone. Coastal Engineering 10, 325-340.

Thornton, E.B., Humiston, R.T., Birkemeier, W., 1996. Bar/trough generation on a natural beach. Journal of Geophysical Research 101, 12097-12110.

Torrence, C., Compo, G.P., 1998. A practical guide to wavelet analysis. Bulletin of the American Meteorological Society 79, 1-78.

Turner I.L., Anderson, D.J., 2007. Web-based and 'real-time' beach management system. Coastal Engineering 54, 555-565.

van Enckevort, I.M.J., Wijnberg, K.M., 1999. Intra-annual changes in bar plan shape in a triple bar system. In: Proceedings of Coastal Sediments '99, New York,1094-1108.

van Enckevort, I.M.J., Ruessink, B.G., 2003. Video observations of nearshore bar behaviour. Part 1: Alongshore uniform variability. Continental Shelf Research 23, 501-512.

van Enckevort, I.M.J., Ruessink, B.G., Coco, G., Suzuki, K., Turner, I.L., Plant, N.G., Holman, R.A., 2004. Observations of nearshore crescentic sandbars. Journal of Geophysical Research 109, pp. *-**. DOI:10.1029/2003JC002214.

Wijnberg, K.M., 1997. On the systematic offshore decay of breaker bars. In: Proceedings of the 25th International Conference, ASCE, New York, 3600-3613.

Wright, L.D., Short, A.D., 1984. Morphodynamic variability of surf zones and beaches: A synthesis. Marine Geology 56, 93-118.

Wright, L.D., Chappell, J., Thom, B.G., Bradshaw, M.P., Cowell, P., 1979. Morphodynamics of reflective and dissipative beach and inshore systems: Southeastern Australia. Marine Geology 32, 105-140.

.

VITA

Name: Gemma Elizabeth Barrett

Address: 810 Eller O&M Building
3147 TAMU
College Station, TX 77843

Email Address: gembarrett@gmail.com

Education: B.S., Environmental Geosciences, Texas A&M University, 2009
M.S., Geography, Texas A&M University, 2011